ABSTRACT

KEITH, ELINOR WHITNEY. Analysis and Prediction of Atlantic Tropical Cyclone Activity. (Under the direction of Lian Xie).

This work begins with the development of a statistical prediction model of numbers of tropical storms, hurricanes and major hurricanes per year in several regions of the Atlantic: the entire Atlantic, the Caribbean Sea and the Gulf of Mexico, as well as landfalling storms along the US Gulf of Mexico, Southeast and Northeast coasts. The methodology involves of cross-correlating variables against Empirical Orthogonal Functions (EOFs) of the Hurricane Track Density Function (HTDF) to select predictors.

The model performs well in the basin-wide predictions over the entire Atlantic and Caribbean, with the predictions showing an improvement over climatology and random chance at a 95% confidence level. Over the Gulf of Mexico, only named storms showed that level of predictability. Predicting landfalls proves more difficult, and only the prediction of named storms along the US Southeastern and Gulf Coasts shows an improvement over random chance at the 95% confidence level. Tropical cyclone activity along the U.S. Northeastern Coast is found to be unpredictable in this model; with the rarity of events, the model is unstable.

In order to provide some physical basis for many of the connections found statistically, the second section is a case study of the 2004-07 Atlantic hurricane seasons. It is found that 2005 had the most favorable SST and vertical wind shear conditions over the main development region. 2004 and 2006 had intermediate levels of SST and wind shear and, outside of the month of August, similar levels of activity. Activity in 2007 was generally

suppressed: although more tropical storms formed than in 2006, they were very short-lived. On average, tropical storms in 2007 survived less than 2.5 days.

The strength of the subtropical anticyclone is a very important factor: in 2005, a weak subtropical high allowed for unusually high SST in the main development region, while in 2007 a strong subtropical high over the east Atlantic cooled SST and increased vertical wind shear. The strength of the subtropical cyclone may be related to the heat release of the African monsoon. This finding also emphasizes the importance of factors relating to the strength of the subtropical high pressure in hurricane prediction.

Analysis and Prediction of Atlantic Tropical Cyclone Activity

by
Elinor Whitney Keith

A thesis submitted to the Graduate Faculty of
North Carolina State University
In partial fulfillment of the
Requirements for the degree of
Master of Science

Marine, Earth and Atmospheric Science

Raleigh, North Carolina

2008

APPROVED BY:

_____ _____

Dr. Lian Xie
Committee Chair

Dr. Anantha Aiyyer

_____

Dr. Montserrat Fuentes

DEDICATION

To my grandfather, Nat Robertson, and all my family. Thank you for supporting me through thick and thin.

I also want to thank my advisor Dr. Lian Xie and committee members Dr. Montserrat Fuentes and Dr. Anantha Aiyyer. Your advice has been invaluable.

BIOGRAPHY

Elinor W. Keith was born in 1982 in New York City and grew up in Athens, Georgia. Her Bachelor's degree from Princeton University was in Geosciences, specializing in Physical Oceanography, was completed in 2004. Her masters from North Carolina State is in Marine, Earth and Atmospheric Science with a minor in Statistics. She will begin Peace Corps service teaching secondary science in Mozambique.

ACKNOWLEDGMENTS

Chapter 1: This study is partially supported by U.S. Department of Energy Grant #DE-FG02-07ER64448 and U.S. National Oceanic and Atmospheric Administration (NOAA) Grant # NA06OAR4810187.

Chapter 2: This work was supported by Department of Energy (DOE) Climate Change Prediction Program grant ER64448, awarded to North Carolina State University.

TABLE OF CONTENTS

LIST OF TABLES

LIST OF FIGURES

INTRODUCTION

Motivation

Hurricanes have caused both the deadliest and most costly natural disasters in US history (Emanuel 2003; Blake et al 2007.) Due to increasing wealth and population along the coast, the US is projected to have one hurricane costing more than $10 million 1995 dollars every six years (Pielke and Landsea 1998.) Rising sea surface temperatures due to global warming may also lead to more very powerful hurricanes (Emanuel 2005; Webster 2005.)

Many sectors of society could benefit from an improved understanding of how tropical cyclone risk varies from year to year. Two major potential end-users are insurance and industries with large energy needs. Typically, insured loses are believed to be roughly half of the total financial losses form a hurricane (Knabb et al. 2005.) When a hurricane passes over the Gulf of Mexico, its effect can be felt around the country because of oil rigs. Jet fuel is the second largest expense for airlines such as Southwest, behind salaries. By buying oil futures, companies can protect themselves against oil shocks (Sullivan, L., 2000.) When fuel costs soared following Hurricanes Katrina and Rita in 2005 (the cost per gallon increasing by 58% year-over-year), Southwest saved dramatically by having 85% of its oil supply capped at $26 a barrel. While the next-highest earner, Continental, managed a net profit of $61 million, Southwest netted $226 million in the third quarter of 2005 (Bond, D., 2005).

CHAPTER 1: Predicting Atlantic Tropical Cyclone Seasonal Activity in April

Predicting Atlantic Tropical Cyclone Seasonal Activity in April

Elinor Keith and Lian Xie*

Department of Marine, Earth and Atmospheric Sciences
North Carolina State University
Raleigh, North Carolina 27695-8208

Submitted to

Journal of Climate

January 2, 2008

* Corresponding author address: Lian Xie, Department of Marine, Earth and Atmospheric Sciences, North Carolina State University, Box 8208, Raleigh, NC 27695-8208. Email: xie@ncsu.edu.

Abstract

Seasonal hurricane forecasts are continuing to develop skill, although they are still subject to large uncertainties. This study uses a new methodology of cross-correlating variables against Empirical Orthogonal Functions (EOFs) of the Hurricane Track Density Function (HTDF) to select predictors. These predictors are used in a regression model for forecasting seasonal named storm, hurricane and major hurricane activity in the entire Atlantic, the Caribbean Sea, and the Gulf of Mexico. In addition, a scheme for predicting landfalling tropical systems along the U.S. Gulf of Mexico, Southeastern, and Northeastern coastlines is developed, but predicting landfalling storms adds an extra layer of uncertainty to an already complex problem, and on the whole these predictions do not perform as well.

The model performs well in the basin-wide predictions over the entire Atlantic and Caribbean, with the predictions showing an improvement over climatology and random chance at a 95% confidence level. Over the Gulf of Mexico, only named storms showed that level of predictability. Predicting landfalls proves more difficult, and only the prediction of named storms along the US Southeastern and Gulf Coasts shows an improvement over random chance at the 95% confidence level. Tropical cyclone activity along the U.S. Northeastern Coast is found to be unpredictable in this model; with the rarity of events, the model is unstable.

Keywords: Hurricane, tropical cyclone, prediction, interannual variability, statistical model

1. Introduction

Many climatic factors are used in predicting the level of tropical cyclone activity of a hurricane season. SSTs in regions hurricanes pass over correlate well with hurricane activity and, given the high heat capacity of the ocean, have longer lead times than many atmospheric indicators. Emanuel (1987, 1991) describes a hurricane as an environmental heat engine driven by sensible and latent heating from the ocean, and therefore very dependent on high SSTs. Goldenburg et al. (2001) shows how the Atlantic Multidecadal Oscillation (AMO), an index based on North Atlantic SSTs, both provides energy directly to hurricanes through higher SSTs and decreases vertical wind shear (VWS), a factor detrimental to hurricanes. Since 1995 the Atlantic has been in its active AMO phase, as shown by the increase in storms between the 1970-1994 period and the 1995-2000.

Wang et al. (2006) found that both the Atlantic Warm Pool (the Atlantic portion of the Western Hemisphere Warm Pool, the area of SSTs > 28.5°C) and Tropical North Atlantic (TNA; SST anomalies over 6°-20°N, 60°-15°W) SSTs correlate with hurricane activity. Knaff (1997) proposed that high Tropical Atlantic SSTs result in lower sea level pressure (SLP), which reduces vertical wind shear and moistens the mid-tropospheric air.

SSTs in other regions may have an impact as well. Xie et al. (2005a) finds that the Atlantic Dipole Mode (DM), the difference between TNA and Tropical South Atlantic (TSA) SSTs affects hurricane activity in three ways. First, as described above, hurricane activity is positively correlated with TNA because high sensible and latent heat availability, low sea level pressure, and small vertical wind shear over the main development region will help

generate more storms. The combination of TNA and TSA also help control the weather of western Africa and tropical and subtropical circulation patterns across the Atlantic.

A similar index to the DM is the Atlantic Meridional Mode (AMM,) which is the result of a maximum covariance analysis of SSTs and the zonal and meridional winds over the region (21°S-32°N, 74°W-15°E; Chiang and Vimont 2004.) However, this coupled mode may offer more insight into the conditions affecting hurricane development than SST conditions alone (Kossin and Vimont 2007.) The AMO can excite the AMM on longer time scales. AMM may even cause the linkage between AMO and hurricane activity (Vimont and Kossin 2007.)

Another important factor is El Niño-Southern Oscillation (ENSO). During La Niña, convection over the eastern tropical Pacific is reduced. This in turn leads to easterly upper tropospheric wind anomalies over the Atlantic. Given that the climatological winds at that height are westerly, these anomalies reduce the VWS (Gray 1984). VWS over the main development region (MDR) between 10°N-20°N from Africa to the Americas can significantly reduce hurricane activity (Gray 1990). Gray (1984) finds that there are an average of 10.9 hurricane days during El Niño years and 23.2 hurricane days during non-El Niño years. Out of the 54 major hurricanes which made landfall over the U.S. from 1900-76, only four happened during the 16 strong to moderate El Niño years. There is an average of 0.25 major hurricane strikes in El Niño years during 1900-83, compared to 0.74 in non-El Niño years. Bove et al. (1998) revisits the issue with updated data and found that the probability of two or more hurricanes making landfall along the U.S. coast is 28% in El Niño

years, 48% during Niño-neutral years, and 66% during La Niña years. Smith et al. (2007) corroborates these differences between ENSO cold and warm years, but found that the situation is more complicated during ENSO-neutral years. The Florida and Gulf coasts experience nearly as many hurricanes during Niño-neutral years as during La Niña years, but along the U.S. East coast from Georgia-Maine, neutral years act more like El Niño years with a large decrease in the number of hurricanes.

The North Atlantic Oscillation (NAO) and the strength of the Atlantic subtropical high may also influence hurricane activity and tracks. Knaff (1998) finds the strength of the subtropical anticyclone over the eastern Atlantic to be a useful for predicting for summertime Caribbean sea level pressure anomalies in April. Sea level pressure anomalies should relate to the potential for tropical cyclone development. Elsner (2003) states that straight-moving hurricanes (which are more likely to make landfall) are more common in years with negative NAO anomalies than positive ones. A negative NAO corresponds to a weaker than normal subtropical high pressure over the eastern Atlantic.

Chelliah and Bell (2004) studied both the Tropical Multidecadal Mode (TMM) and ENSO. They found the TMM to be even more important than ENSO in determining the upper tropospheric winds. TMM and ENSO combined accounted for 70-80% of the variance of the 200 hPa velocity anomalies between 30ºS-30ºN. TMM is found to represent 50-60% of the overall variability, with ENSO contributing 22-24%. Negative TMM and La Niña conditions both tend to reduce shear over the tropical Atlantic.

The negative-phase TMM (an active multidecadal mode) is also associated with

anomalous upper-level divergence and increased rainfall over Africa (Chelliah and Bell 2004). The plentiful African rainfall is in turn associated with increased Atlantic hurricane activity and, in particular, greater landfall of intense hurricanes in the U.S., especially over Florida (Gray 1990).

This paper is organized into five sections. In section 2 the hurricane data and atmospheric and oceanic predictors are described. Section 3 contains the methodology used in: (a) computation of the Hurricane Track Density Function (HTDF), (b) its decomposition into EOFs, (c) the use of those EOFs to select variables for the final hurricane prediction, and (d) validation of the final regression model. Section 4 describes the results, subdivided into (a) the description of HTDF EOF results, (b) the final predictors selections, (c) model validation, and (d) 2007 predictions and validation. Section 5 contains conclusions and remarks.

2. Data

The hurricane and tropical storm data come from the "best-track" database (HURDAT), maintained by NOAA's National Hurricane Center (NHC). This data set contains 6-hourly storm locations for all tropical storms and hurricanes from 1851-2005. Because of large uncertainties in the earlier data, the analysis is limited to data from 1944-2007, during the period of airplane tracking . Subtropical and extratropical storms, as well as storms outside of the June 1-November 31 hurricane season are filtered out. Landfalling hurricanes in the U.S. are listed in the record along with their category at landfall and the state in which it occurred. Landfalling tropical storms had to be counted separately; only those tropical storms passing from water onto land are taken as landfalling. Gulf of Mexico landfalling storms are those making landfall along the U.S. coast from the Texas-Mexico border to the southern tip of Florida. The southeastern coast is from this point north to the North Carolina-Virginia border. The northeast region is from Virginia through Maine.

The regression of tropical storm-force winds is fit using Extended Best Track Data (Demuth et al. 2006) available at http://rammb.cira.colostate.edu/research/tropical_cyclones/tc_extended_best_track_dataset/.

The data indices used as predictors of hurricane activity come from several sources. AMO Index is available from the Climate Prediction Center (CPC) at http://www.cdc.noaa.gov/ClimateIndices/List/ and is based on Enfield et al. (2001). AMM is available at http://www.cdc.noaa.gov/Timeseries/Monthly/AMM/amm.data (Chiang and

Vimont 2004.)

DM is computed using Extended Reconstructed SST (ERSST) data (Smith and Reynolds 2004) and is the normalized area average SST of the North Tropical Atlantic (4ºN-24ºN, 60ºW-15ºW) minus the South Tropical Atlantic (15ºS-30ºS, 30ºW-12ºE) normalized area averaged SST.

NAO is calculated using rotated principle component analysis and is available from CPC at http://www.cdc.noaa.gov/Correlation/nao.data.

The Niño 1+2 index is available from CPC at http://www.cpc.ncep.noaa.gov/data/indices/sstoi.indices. Niño 1+2 forecasts are based on the NCEP Climate Forecast System (Saha et al. 2006) and available at http://www.cpc.noaa.gov/products/analysis_monitoring/lanina/ensoforecast.shtml.

TNA and TSA are available from PSD and AOML at http://www.cdc.noaa.gov/ClimateIndices/List/ and are based on Enfield et al. (1999). WHWP is available from PSD and AOML at http://www.cdc.noaa.gov/ClimateIndices/List/ and climatology is from Wang and Enfield (2001). Data analysis is done in R (R Development Core Team, 2006) using the extra packages MASS (Venables and Ripley 2002), and Verification by NCAR - Research Application Program.

3. Methods

a. Hurricane Track Density Function (HTDF)

The Hurricane Track Density Function (HTDF) is based on the cyclone track density function of Anderson and Gyakum (1989), and is a way of converting track data from discrete storms into a regular grid in time and space. The cyclone track density field, C(**x**, t), is defined as:

$$C(\mathrm{x},t) = \sum_j W(\mathrm{x}-\mathrm{x}_j, t-t_j)$$

$$W(\Delta \mathrm{x}, \Delta t) = \begin{cases} \cos^2 \dfrac{|\Delta \mathrm{x}|}{S_x} \cos^2 \dfrac{|\Delta t|}{S_t} & \textit{if } \dfrac{|\Delta \mathrm{x}|}{S_x} < \dfrac{\pi}{2} \textit{ and } \dfrac{|\Delta t|}{S_t} < \dfrac{\pi}{2}; \cdot \\ 0 & \textit{otherwise}; \end{cases} \quad (1)$$

The variable $\boldsymbol{x_j}$ is defined as the *j*th cyclone observation taken at time t_j, and the grid point being estimated is at position ***x*** and time *t*. W(Δ***x***, Δ*t*) is a weighting function for the interpolation (Anderson and Gyakum 1989; Xie et al. 2005b.)

In this study the function is modified to better represent the probability of tropical storm-force winds, based on an extension of the regression model described in Kossin et al. (2007), where radius of tropical storm-winds (R34) are estimated based on maximum wind speed, latitude, and storm age. However, examination of the dependent variable and regression residuals showed that the data are right-skewed and could benefit from a transformation to improve normality. The Box-Cox method is designed to find the transformation which would leave the data closest to normality (Box and Cox 1964.)

Table 1: SAS proc transreg output used to find the Box-Cox transform in the regressions on radii of tropical storm- and hurricane-force winds. The italicized values mark the maximum log-likelihoods with the 95% confidence region in bold. Typically, a convenient value within this confidence region is used. In this case, ⅓ is used for R34.

λ	R34 regression R^2	R34 log-likelihood
0	0.45	-20136.9
0.05	0.45	-20082.3
0.1	0.46	-20036.7
0.15	0.46	-20000
0.2	0.46	-19971.9
0.21	0.46	-19967.3
0.22	0.46	-19963
0.23	0.46	-19959.1
0.24	0.46	-19955.5
0.25	0.46	-19952.3
0.26	0.46	-19949.4
0.27	0.46	-19946.8
0.28	0.46	-19944.5
0.29	0.46	-19942.6
0.3	0.46	-19941
0.31	0.46	-19939.7
0.32	**0.46**	**-19938.7**
0.33	**0.46**	**-19938.1**
0.34	**0.46**	**-19937.8**
0.35	***0.46***	***-19937.8***
0.36	**0.46**	**-19938.1**
0.37	**0.46**	**-19938.7**
0.38	**0.46**	**-19939.6**
0.39	0.46	-19940.9
0.4	0.46	-19942.4
0.45	0.46	-19954.8
0.5	0.46	-19974.6
0.55	0.46	-20001.7
0.6	0.46	-20035.7
0.65	0.46	-20076.6
0.7	0.45	-20124.1
0.75	0.45	-20178
0.8	0.45	-20238.1
0.85	0.44	-20304.1
0.9	0.44	-20375.8

Table 1 (Continued)

λ	R34 regression R^2	R34 log-likelihood
0.95	0.44	-20453.1
1	0.43	-20535.8

Box-Cox transforms are of the form:

$$y^{\lambda} = \begin{cases} \dfrac{y^{\lambda} - 1}{\lambda} & \lambda \neq 0 \\ \ln(y) & \lambda = 0 \end{cases} \tag{2}$$

Using SAS proc transreg, we found a transformation which maximized the log-likelihood to be $\lambda = \frac{1}{3}$ for R34 (Table 1.) The final Box-Cox transform is:

$$R34_{BC} = \frac{(\sqrt[3]{R34} - 1)}{1/3} \tag{3}$$

The final regression model for the radius of tropical storm-force (R34) winds in kilometers is:

$$R34_{BC} = 6.56 + 0.0599 \cdot Vmax + 0.0912 \cdot lat + 0.00846 \cdot age + \varepsilon \quad \hat{\sigma}_{\varepsilon} = 2.273 \quad MAE = 55.36 \tag{4}$$

where V_{max} is the storm's maximum wind speed in knots at that time, φ is the latitude in degrees, and Δt is the storm age in hours. ε is the error, with standard deviation ($\hat{\sigma}_{\varepsilon}$) here is shown relative to the transformed variables and is the square root of the PRESS statistic divided by the degrees of freedom. The mean absolute error (MAE) has been converted back to km for comparison. These errors are slightly higher than those reported in Kossin et al. (2007): 50.3 km for R34, perhaps due to the use of different record periods. However, the increased normality is important for generating the probabilities used in this study.

The output of the regression equations in (4) are the expected values, $E[R34_{BC}]$, of the transformed variables $R34_{BC}$. They can be converted into the standard normal distribution using the equations:

$$D_{34} = \frac{\sqrt[3]{distance} - 1}{1/3}$$
$$z_{34} = \frac{D_{34} - E[R34_{BC}]}{\hat{\sigma}_{\varepsilon}} \quad (5)$$

The probability P of tropical storm- winds at a grid point can be calculated from the standard normal probability distribution between by:

$$P = 1 - (\frac{1}{\sqrt{2\pi}} \int_{-\infty}^{x} \exp^{\frac{-z^2}{2}} dz) = 1 - \frac{1}{2}(1 + erf(\frac{z}{\sqrt{2}})) \quad (6)$$

where *erf()* is the error function. This equation is one minus the probability that the true radius of storm winds is less than the distance between the grid point and the storm center.

A diagram of the HTDF process is shown in Figure 1, with an example of calculating the probability of tropical storm-force winds from Hurricane Dennis (2005) at three grid points on Jul 7, 2005. Given a day's track of some tropical cyclone and the location of a grid point, the algorithm will first compute when and where the track passes the closest to the grid point and the distance between the two. Next, it finds what the latitude (lat), maximum wind speed (Vmax), and age of the storm would be at that closest location, interpolating between observations as necessary. Then using Eq. 4-6 the probability of tropical storm-force winds from the tropical cyclone is calculated at the grid point. This process continues via a brute force approach: repeatedly matching every day of every storm with each grid point.

In this study, the HTDF is calculated on a 1°x 1° grid between 10°N-40°N and 50°W-100°W. Grid points over land, the Great Lakes, and the Pacific are removed. The decision to

exclude the eastern-most portion of the basin reflects several factors. Much of the model is focused on performance predicting landfalls and tropical cyclones over the Gulf of Mexico and Caribbean in the western Atlantic. Excluding points also reduces computation time dramatically given that the program is brute force and runs in $n_d * n_x * n_y$ time, where n_d is the number of days with storms and n_x and n_y are the number grid points in x and y, respectively. The time domain is daily over the 183-day hurricane season (June 1-November 30) from 1944 through 2007 (64 years of data).

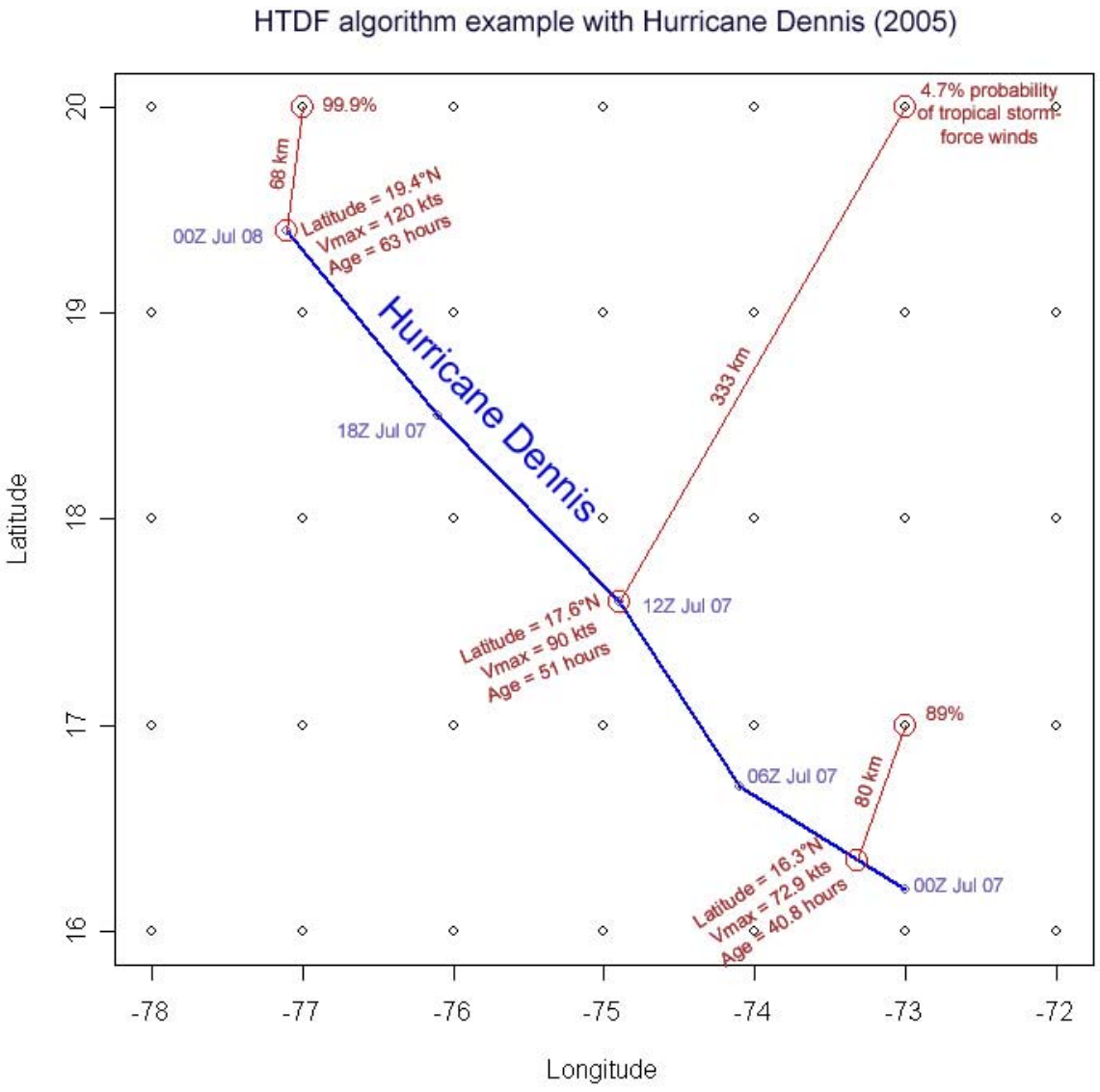

Figure 1: An HTDF algorithm example for the grid points at (20°N, 77°W), (20°N, 73°W) and (17°N, 73°W) with Hurricane Dennis on Jul 7, 2005. The algorithm takes the five track points for 00Z of the current y through 00Z of the following day and locates the closest geographic point along the four line segments connecting them. A subroutine returns the distance from the line segment to the point along with the storm latitude, Vmax and age, interpolated between observations as needed. This procedure is repeated matching every day of every track with every grid point.

b. Empirical Orthogonal Functions (EOFs)

The probabilities generated by the HTDF are then used to generate EOFs by singular value decomposition (SVD). EOFs are described in Lorenz (1956) and are commonly used in meteorological and oceanic data analysis (e.g., Richman and Lamb 1985; Xie et al. 2005b.) Should each of the largest eigenvectors correspond to physical factors, those factors would make a valuable predictor of hurricane activity.

Richman and Lamb (1985) assert the importance of factor rotation in order to generate more robust spatial patterns. To address this, VARIMAX rotation is used but made an insignificant difference (When the top four EOFs are rotated, the Pearson correlations between the unrotated and rotated R34 EOF spatial loadings are all greater than 0.9). To further test the stability of the patterns a Monte Carlo simulation is run with 100 iterations each using 25-75% of the total number of storms in the dataset. The spatial correlations of each of these results in the case of the R34 EOFs are greater than 0.9 in 100 out of 100 trials for each of the top three EOFs. The results for the R64 are not nearly as strong. For the first three EOFs only 83, 58, and 21 out of 100 iterations had correlations over 0.9. Even using a lower correlation threshold of 0.85, 90, 72, and 38 of the first three EOFs are repeated. This analysis has also been attempted on the radius of hurricane-force winds, but they are not very stable with varying the subsets of the data they will not be used in the final analysis.

c. Selection of predictors

To select the predictors, the EOF time series are averaged by month. Cross-correlations between these monthly EOF time series and a large set of monthly atmospheric and oceanic indices are computed. Aside from El Niño, predictors are required to have correlations significant at least at the 95% level over a period of at least two months with a minimum lead time of four months. In the case of El Niño, the index is still required to be significant for at least two months, but there is no requirement of lead time. El Niño predictions can be used in the final model.

In cases where the Spearman correlation between indices is high, the indices are likely to be reflecting the same physical factor. Here, a set of five variables (AMM, AMO, DM, TNA and WHWP) show significant inter-correlation. In the presence of collinearity, principle components regression is one way to reduce the variance of the regression coefficients and reduce the mean squared error (Rawlings et al. 2001.) It also has the benefit of striking a balance between incorporating the information in all the variables and avoiding over-fitting the data. In the final regression, the first principle component (PC) of the AMM, AMO, DM, TNA and WHWP is used in place of the five variables.

d. Model validation

These final models are evaluated using both leave-one-out cross-validation (LOOCV) and by testing how well the model predicts for the later years of data without that data being included in the initial model. Both of these methods are preferable over simple tests of fit

because they more effectively protect against over-fitting. However, in order to check that the methodology is not simply selecting for variables which are only coincidentally related and maintain the accuracy of cross-validation statistics, a variable selection approach such as stepwise selection would need to be redone within each cross-validation repetition as well. Cross-validation must test the methodology rather than just the final result (Elsner and Schmertmann 1994). The variables need to be determined by the EOF analysis rather than in the regression itself.

Table 2: Spearman correlations between predictors

	AMM (Jan-Feb)	AMO (Jan-Feb)	DM (Jan-Feb)	Niño1+2 (Jul-Aug, predicted)	TNA (Jan-Mar)	TSA (Oct-Dec)	WHWP (Aug-Nov)	Principle component
AMM	1.00	**0.68**	**0.77**	-0.04	**0.82**	-0.21	0.47	**0.94**
AMO	**0.68**	1.00	**0.56**	-0.17	**0.67**	0.10	**0.71**	**0.81**
DM	**0.77**	**0.56**	1.00	0.04	**0.74**	-0.23	0.27	**0.74**
Niño 1+2	-0.04	-0.17	0.04	1.00	-0.06	-0.39	-0.34	-0.13
TNA	**0.82**	**0.67**	**0.74**	-0.06	1.00	0.06	**0.62**	**0.87**
TSA	-0.21	0.10	-0.23	-0.39	0.06	1.00	0.41	-0.01
WHWP	0.47	**0.71**	0.27	-0.34	**0.62**	0.41	1.00	**0.72**
Principle component	**0.94**	**0.81**	**0.74**	-0.13	**0.87**	-0.01	**0.72**	1.00

The forecast skill is judged using the ranked probability skill score (RPSS), which stringently measures the reliability of probabilistic forecasts relative to climatology or some other baseline (Goddard et al. 2003; Epstein 1969). In order to compute the RPSS, individual forecasts are assigned a ranked probability score (RPS):

$$RPS = \sum_{m=1}^{N_{cat}} (CP_{F_m} - CP_{O_m})^2 \tag{7}$$

where N_{cat} is the total number of categories, CP_{Fm} is the cumulative forecast probabilities up to category m, and CP_{Om} is the cumulative observed probability up to category m (i.e., CP_{Om} = 1 if the observed category is less than or equal to m, and CP_{Om} = 0 otherwise). The RPSS is then:

$$RPSS = 1 - \frac{\sum_{i=1}^{N_{forecast}} RPS_i}{N_{forecast} \times RPS_{ref}} \tag{8}$$

where $N_{forecast}$ is the number of forecasts made, RPS_i is the RPS for the i^{th} forecast, and RPS_{ref} is the baseline RPS value, generally based on climatology (Goddard et al. 2003; WWRP/WGNE Joint Working Group on Verification 2007).

Significance levels are found via Monte Carlo simulation, using 10,000 sets of randomly generated Poisson means from the same distribution as with the actual regression. The RPSS of each set is calculated. The p-value is then one plus the number of RPSSs calculated that are greater than the actual RPSS divided by one plus the number of trials (10,000).

4. Results

a. HTDF EOFs

The top three R34 EOFs explain approximately 22% of the total HTDF on a daily time scale. The percent variance explained for the top 25 EOFs are shown in Figure 2. The cutoff is chosen after the third because at that point the variances drop below 5% and level off. The spatial loading patterns and time series of the EOFs are shown in Figure 3, with the track patterns for the five largest and smallest years of each EOF shown in Figure 4. Tropical storm, hurricane, and major hurricane counts for each set of ten years is shown in Table 3.

EOF1 explains 10.2% of the variance (Figure 2) and its spatial pattern (Figure 3a) is positive over much of the domain and near zero over the Gulf of Mexico. It is maximized off the U.S. eastern coast with loadings greater than 0.65. This pattern will be particularly useful in finding predictors for basinwide activity and landfalls along the northeastern coast. Table 3 shows that approximately one half as many tropical storms, hurricanes and major hurricanes occur throughout the Atlantic during the largest ten years of EOF 1 (EOF1+) than during the smallest ten (EOF1-). The track patterns in Figure 3 further support this, with activity particularly increased in the northern and eastern portions of the domain.

Another 6.2% of the variance is explained by EOF2 (Figure 2), which has large loadings greater than 0.5 off of the U.S. southeastern coast (see Figure 3c). It also has negative loadings further north, indicating that more storms recurve away from the coastline into the northern Atlantic during the negative mode of EOF2. This is visible in Figure 4d,

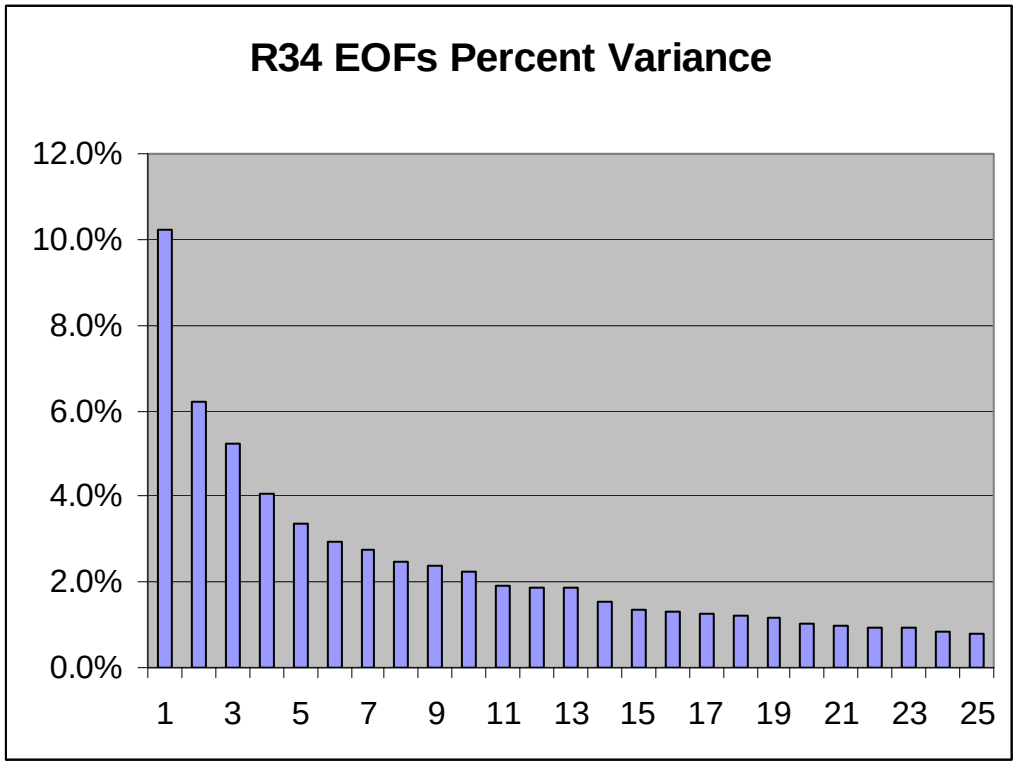

Figure 2: Percent variance explained by the top 25 R34 EOFs. The top 3 EOFs are chosen because after that point the variance explained by each EOF levels off and drops below 5%.

Figure 3: Top 3 R34 spatial loading patterns (a, c, and e) and time series (b, d, and f). The daily time series are average by year here for display. EOF1 (a and b) explains 11% of the variance and its highest spatial loading centers over the north-central part of the domain, and includes many storms recurving into the north Atlantic (see figure 3 for track patterns) as well as those striking the US northeastern coast. EOF2 (c and d), with 6.6% of the variance, is a more southerly spatial pattern, with strongly positive loadings off of the Atlantic coast of Florida. The highest spatial loadings of EOF3 (e and f; 5.4% of the variance) are more southerly still; they are maximized through the Caribbean and Gulf of Mexico.

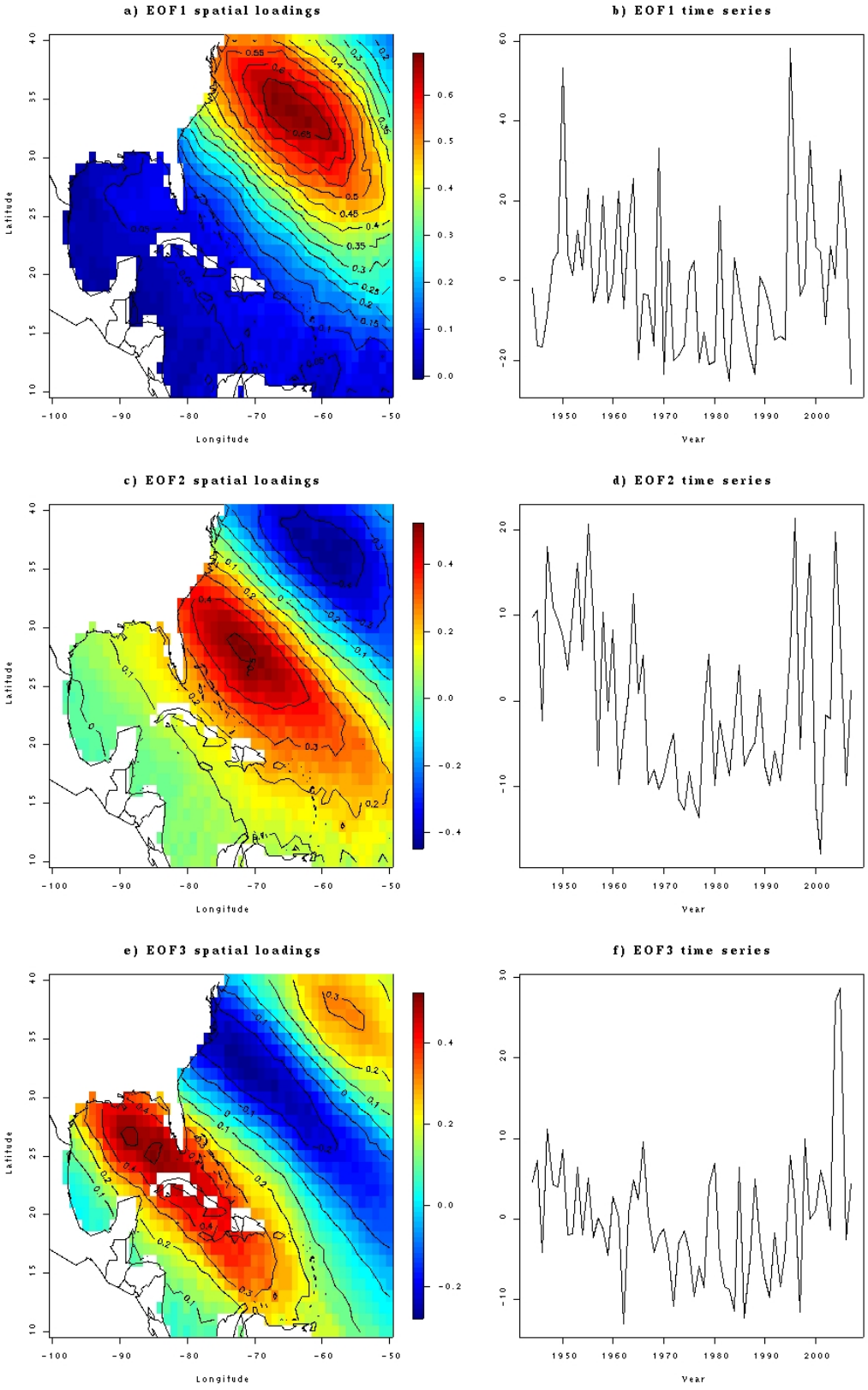
a) EOF1 spatial loadings
b) EOF1 time series
c) EOF2 spatial loadings
d) EOF2 time series
e) EOF3 spatial loadings
f) EOF3 time series
Latitude
Longitude
Year

Figure 4: Track patterns during the five highest (a, c and e) and five lowest (b, d and f) years for the top three R34 EOFs. Tropical storms are shown in violet, category 1 hurricanes in blue, cat. 2 in green, cat. 3 in yellow, cat. 4 in orange, and cat. 5 in red. EOF1 (a and b) is associated with positive activity everywhere in the Atlantic Basin, particularly off the US eastern seaboard. EOF2 (c and d) is largely associated with storms landfalling along the U.S. southeastern coastline from Florida through North Carolina. EOF3 (e and f; 5.4% of variance) predominantly effects the southern and western parts of the domain, in the Caribbean Sea and Gulf of Mexico.

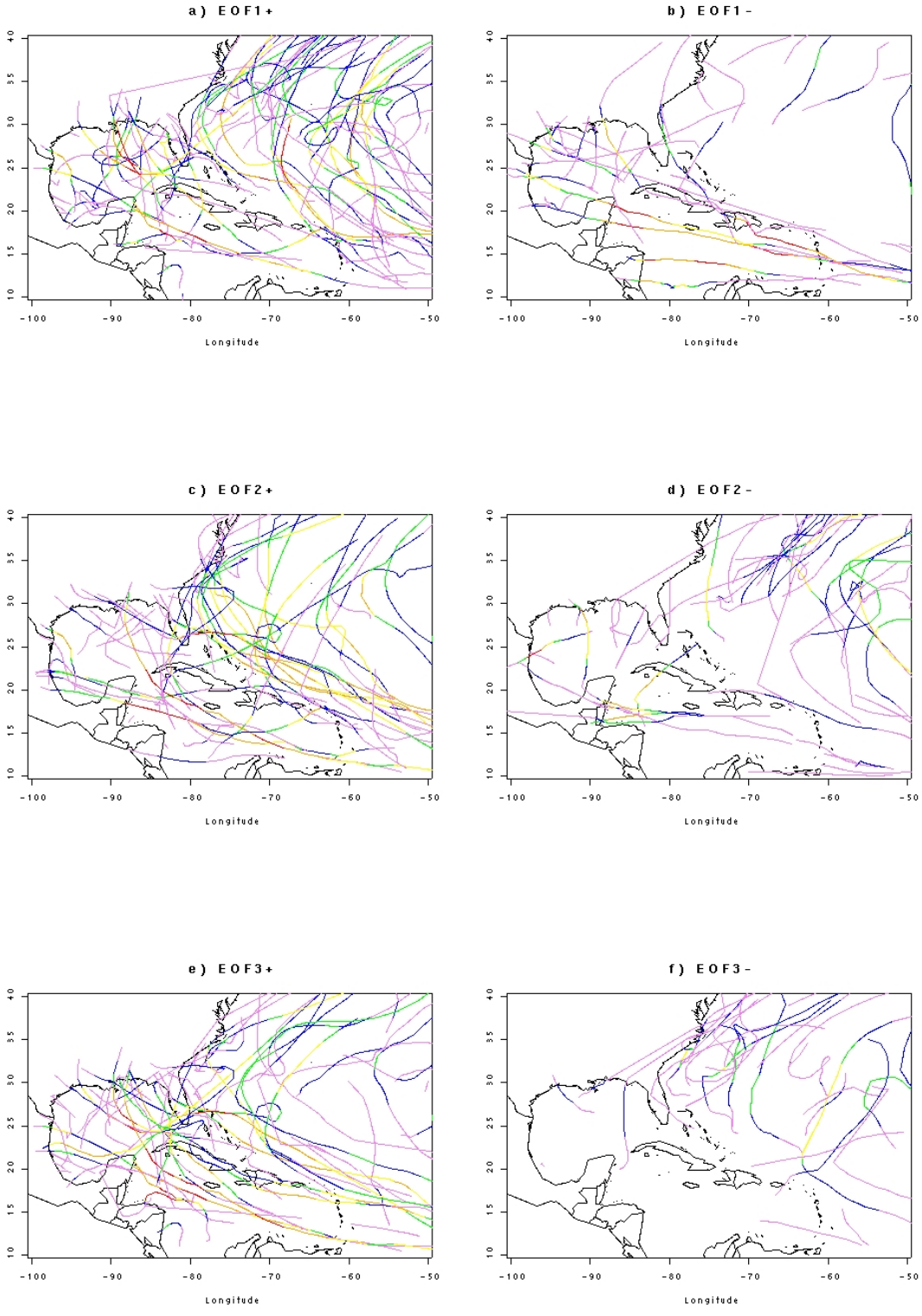
a) EOF1+
b) EOF1-
c) EOF2+
d) EOF2-
e) EOF3+
f) EOF3-
Longitude
-100
-90
-80
-70
-60
-50
10
15
20
25
30
35
40

Table 3: Numbers of basinwide and landfalling Named Storms (tropical storms + hurricanes), Hurricanes (H), and Major Hurricanes (MH) in the ten largest and ten smallest years for each R34 EOF. The EOF mode with the highest spatial loading over a region is highlighted.

Region		EOF1+	EOF1-	EOF2+	EOF2-	EOF3+	EOF3-
Whole Atlantic	TS + Hur	145	80	114	103	141	72
	Hur.	95	48	70	66	87	39
	Maj. Hur.	60	15	47	24	43	11
Caribbean	TS + Hur	43	17	44	21	**41**	**9**
	Hur.	29	7	22	11	**20**	**1**
	Maj. Hur.	17	6	11	7	**12**	**1**
Gulf of Mexico (all storms)	TS + Hur	43	33	41	22	**57**	**13**
	Hur.	27	20	20	10	**30**	**6**
	Maj. Hur.	13	8	10	4	**15**	**1**
Gulf of Mexico (landfalling)	TS + Hur	26	21	32	14	**41**	**8**
	Hur.	15	10	13	4	**20**	**4**
	Maj. Hur.	10	5	6	3	**10**	**1**
Southeast coast	TS + Hur	18	5	**24**	**2**	20	7
	Hur.	13	2	**19**	**0**	15	3
	Maj. Hur.	5	1	**7**	**0**	4	1
Northeast coast	TS + Hur	**6**	**2**	5	4	2	4
	Hur.	**1**	**1**	1	3	1	3
	Maj. Hur.	**0**	**0**	0	0	0	0

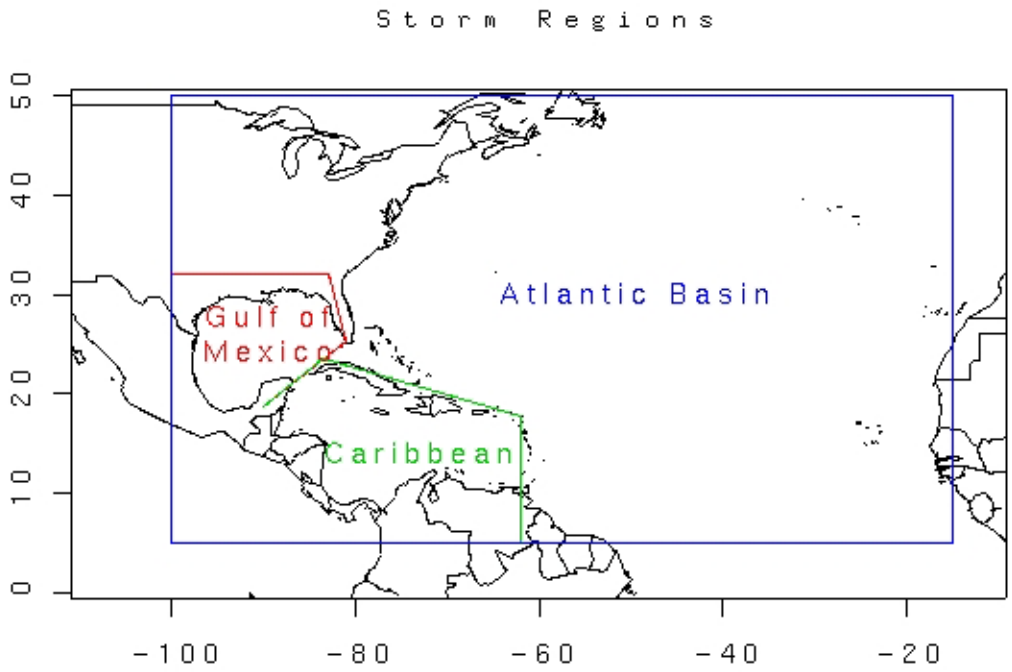

Figure 5: A map of storm regions. Any storm declared a tropical storm or hurricane by the National Hurricane Center counts for the Atlantic Basin. If that storm crosses into the Caribbean Sea or Gulf of Mexico, it is counted for those regions at the highest intensity it reached during that passage. Landfalling storms are grouped into three regions: the U.S. Gulf Coast from Texas through the western coast of Florida, the U.S. southeastern coast, from the east coast of Florida to the North Carolina-Virginia border, and the U.S. northeastern coast from Virginia to Maine.

Table 4: Final model variables.

Region	Independent Variables
Whole Atlantic	Niño1+2 (Jul-Sep), TSA (Nov-Jan), Principle component
Caribbean Sea	Niño1+2 (Jul-Sep), TSA (Nov-Jan), Principle component
Gulf of Mexico	Niño1+2 (Jul-Sep), TSA (Nov-Jan), Principle component
Gulf of Mexico (Texas – West Florida)	Niño1+2 (Jul-Sep), TSA (Nov-Jan), Principle component
Southeast (East Florida-North Carolina)	Niño1+2 (Jul-Sep), TSA (Nov-Jan), Principle component
Northeast (Virginia-Maine)	Niño1+2 (Jul-Sep), Principle component

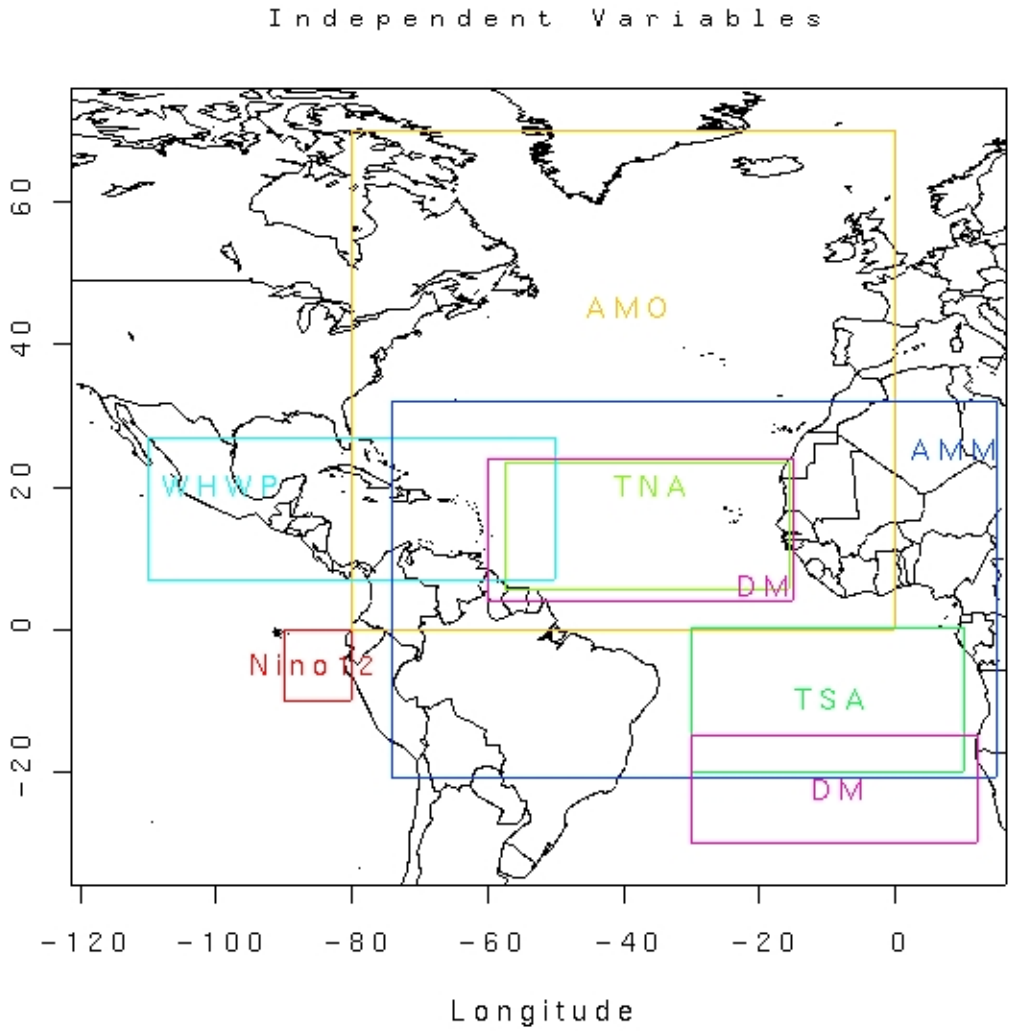

Figure 6: Independent variables with significant cross-correlation with HTDF EOFs. The Atlantic Meridional Mode (AMM) is the Maximum Covariance Analysis of the SST and the 10m wind field over the tropical Atlantic (Chiang and Vimont 2004.) The Atlantic Multidecadal Oscillation (AMO) is the detrended area-weighted SST across the entire North Atlantic (Enfield et al 2001); the Atlantic Dipole Mode (DM) is the standardized SST difference between the North (4°N-24°N, 60°W-15°W) and South (15°S-30°S, 30°W-12°E) tropical Atlantic (Enfield et al 1999; Xie et al 2005a); El Niño 1+2 is the area weighted SST anomaly in the eastern Pacific just off the South American coast; Tropical North Atlantic (TNA) index and the Tropical South Atlantic (TSA) index are the area-weighted SST anomalies in the North and South Tropical Atlantic, respectively (Enfield et al 1999); and the Western Hemisphere Warm Pool (WHWP) is the monthly anomaly of the area of SSTs > 28.5°C, or warm enough to support a hurricane (Wang and Enfield 2001).

where during the EOF 2- years most of the storms present outside of the Caribbean and Gulf of Mexico do recurve away from land. The ten most positive (negative) years had 24 (2) tropical storms, 19 (0) hurricanes, and 7 (0) major hurricanes (Table 3.) Predictors which correlate with this eigenmode should help predict landfalling storms along the southeast and basinwide activity.

EOF3 explains 5.2% of the variance (Figure 2). In Figure 3e, it is maximal with loadings greater than 0.5 in the Caribbean Sea and Gulf of Mexico, negative loadings further north, near the North Carolina coast, and positive loadings in the northeastern corner of the domain. As shown in Figure 4e-f and Table 3, the regions most strongly affected by this EOF mode are the Caribbean Sea and both Gulf of Mexico storms and storms landfalling along the U.S. Gulf Coast. In these regions, the ten largest years have more than four times the tropical cyclone activity of the ten smallest years. EOF 3+ years also exhibit an increase in activity throughout the Atlantic and some increase in storms making landfall along the southeast coast because the increase in storm activity along the Atlantic coast of Florida outweigh the decrease along the North Carolina coast.

b. Predictors

The R34 EOFs are then used to select predictors for the final regression models of tropical cyclone activity. Based on correlations with the top three R34 EOFs, 6 predictors are selected for all the regressions, all of which are mapped in Figure 5. Table 4 shows the final set of variables chosen for each region, based on cross-correlations with the HTDF EOFs.

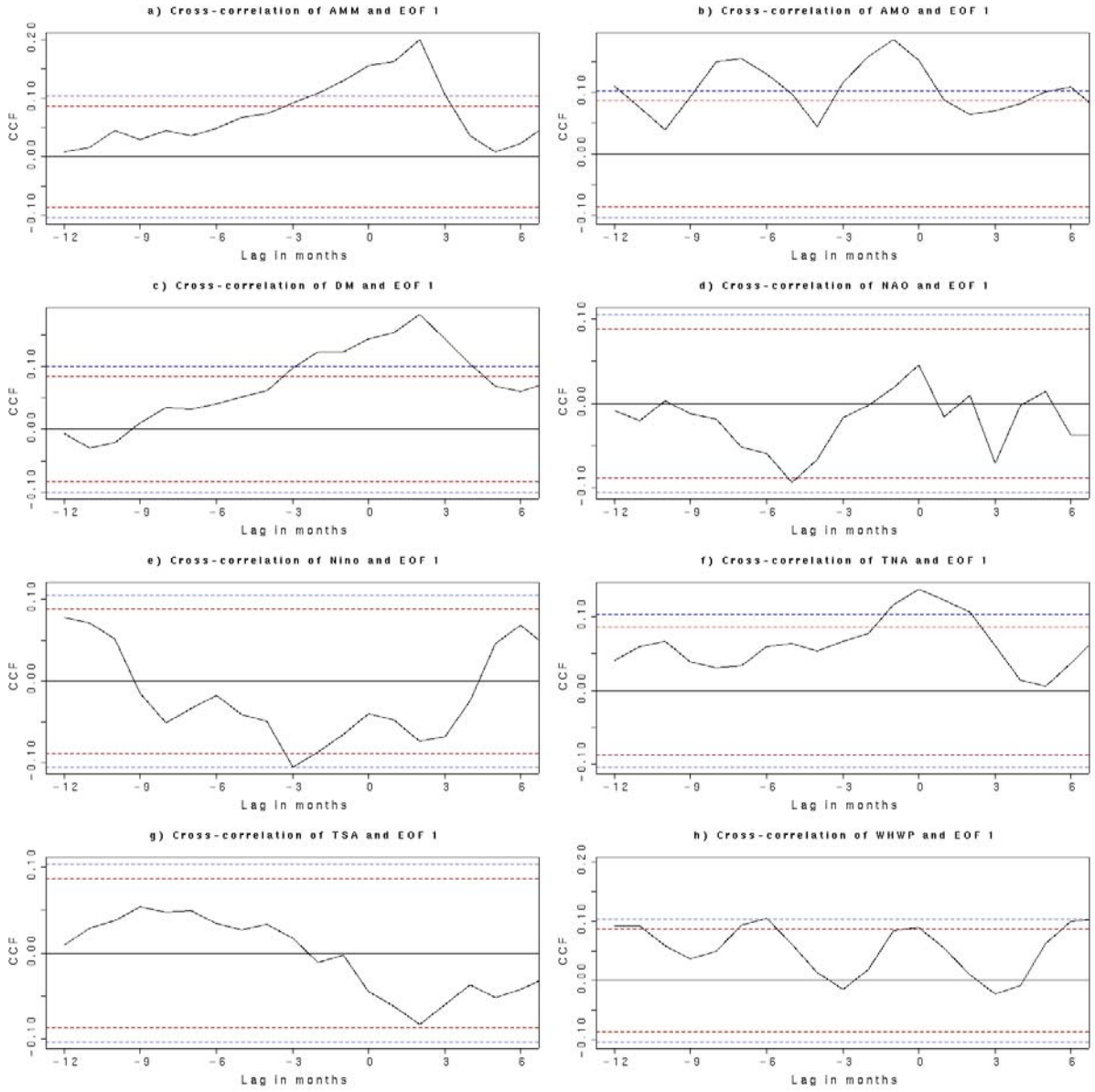

Figure 7: Cross-correlations of the first EOF with eight potential explanatory variables of the HTDF. The variables are (a) AMM, (b) AMO, (c) DM, (d) NAO, (e) Niño 1+2, (f) TNA, (g) TSA and (h) WHWP.

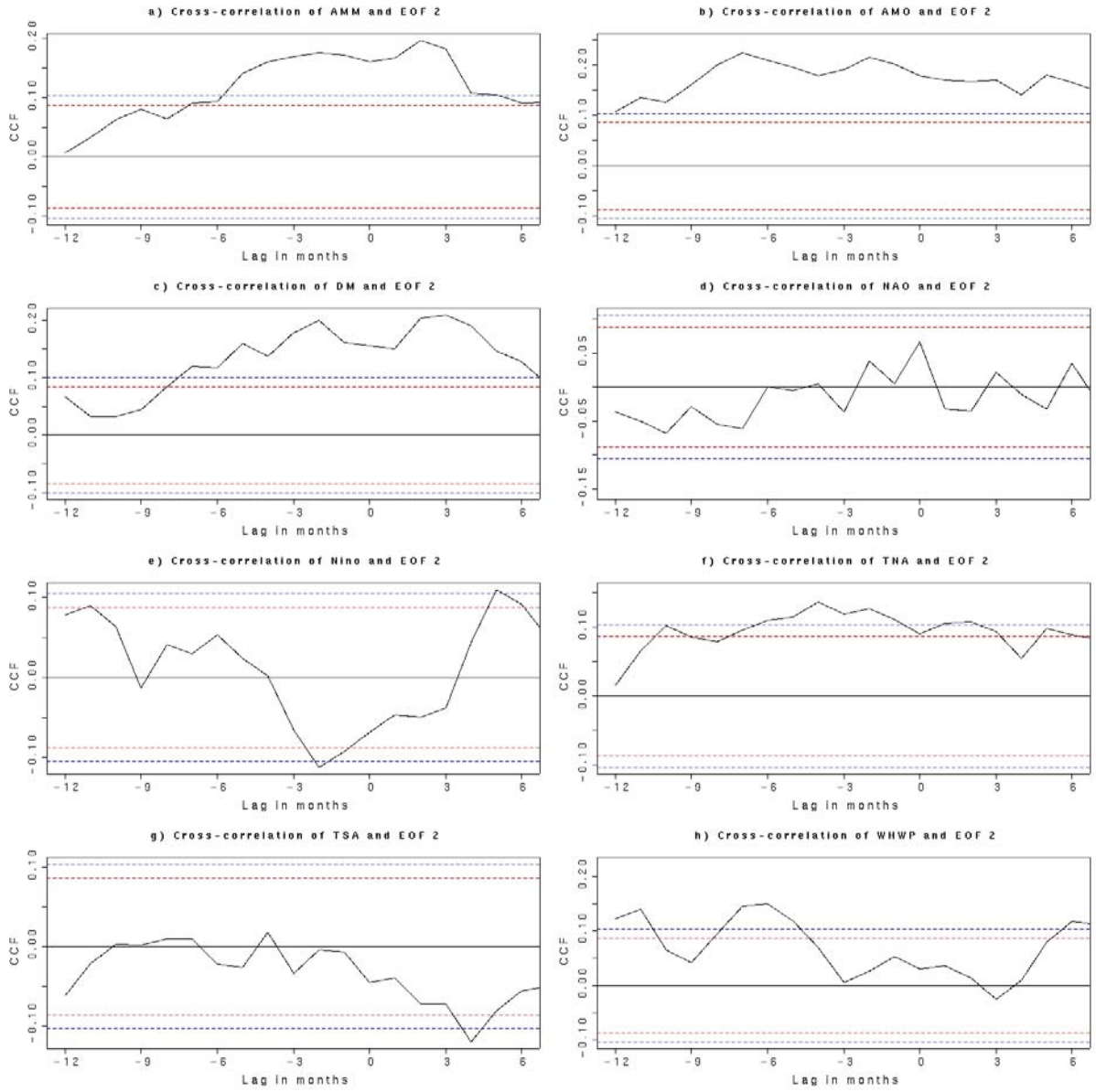

Figure 8: Cross-correlations of EOF2.

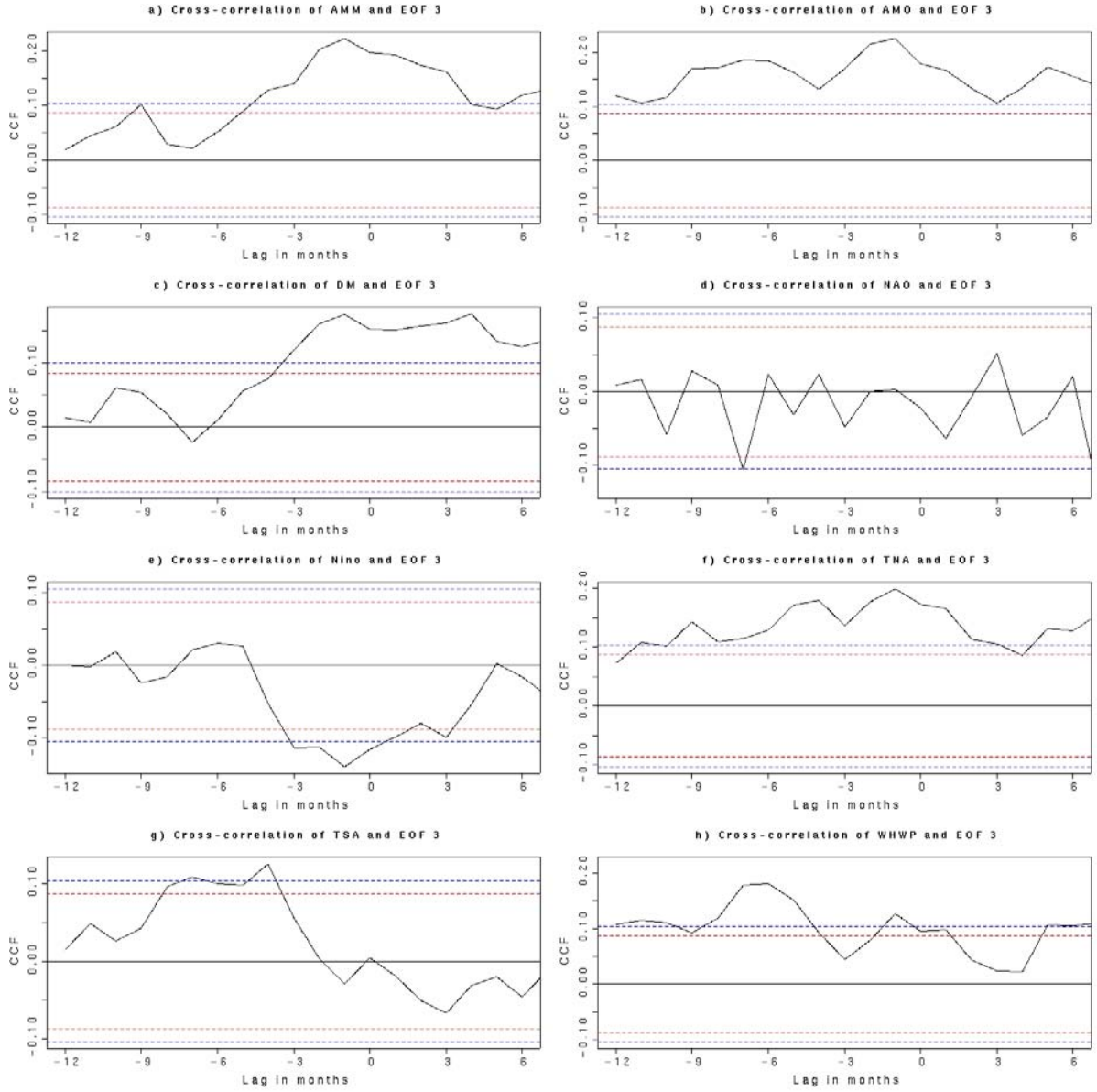

Figure 9: Cross-correlations of EOF3.

Several of the variables which make up the principle component (PC) are significantly correlated with the time series of EOF1 (Figure 7) with at least three month's lead time: AMM, AMO, DM and WHWP. The Niño 1+2 index also shows 95% significant correlation with three months lead. NAO and TSA do not reach 95% significant correlation. Because of this, the PC is used along with Niño 1+2 to predict landfalling tropical cyclones along the Northeast coast.

EOF2 (Figure 8) shows largely the same correlations as EOF1. It correlates significantly with all of the indices making up the PC are significantly correlated. The Niño 1+2 index is correlated as well, and NAO and TSA are not.

All of the indices correlate at a 95% significance level with EOF3, but with NAO only one month is greater than 90% significance, which does not meet the criteria. The other variables are used for predicting over the Gulf of Mexico, Caribbean Sea and entire Atlantic: Niño 1+2, PC and TSA.

c. Model Validation

The next step is to validate the model for how well it predicted actual numbers of tropical storms, hurricanes and major hurricanes based on three sets of tests. Two of those tests, the 1990-2007 and 1980-2007 hindcast, simulated realistic forecasting by only using the earlier years of data to determine regression coefficients then seeing how well the model predicted each year. For example, the 1990-2007 hindcast would first predict the value for 1990 based on data from 1950-1989 to determine coefficients for the 1990 independent

variables. Next it would predict 1991 coefficients based on 1950-1990 data, and so on.

Leave-one-out Cross Validation (LOOCV) works by only leaving out one year at a time (i.e. it would use 1950-1989 and 1991-2007 data to predict for 1990). This method has the benefit of running 56 tests, rather than 27 for the 1980-2007 hindcast, but is not as realistic given that it includes data from later years.

The results of these tests are evaluated in two ways. The simple model validation (Table 5) shows the sum of all of the errors if each year's forecast are given as a range. For example, if the model for Gulf Coast tropical storms one year estimated 3.2 storms, the prediction would be for 3-4 storms. If there are actually 5 storms, the error for that year would be 1. This error can be compared to the deviation from climatology; the error you would get by predicting the average number of storms every year. The regions and types of storms found to be significant in Table 6 also show equal or less error in the model than in climatology.

Table 6 contains a more complete model validation based on the ranked probability skill scores (RPSS) of all of the same tests. P-values are based on Monte Carlo simulation with n = 10,000. The regions with at least two tests at a 95% significance level are in bold.

The best results are for the Atlantic basin as a whole. All nine tests among the three strengths of storms (tropical storms and hurricanes, hurricanes, and major hurricanes) are significant at a 95% level over random chance and all except for the 1990-2006 hindcast for Atlantic hurricanes are significant at a 99% level. The error reductions in Table 5 also show an average of an 18% improvement over climatology.

Table 5: Simple model validation. Bold lines correspond to the variables found in table 4 to have at least two tests significant at the 95%.

Region	Dependent Variable	Error (1990-2007 hindcast)	Deviation from climatology (1990-2007)	Error (1980-2007 hindcast)	Deviation from climatology (1980-2007)	Error (1950-2007 LOOCV)	Deviation from climatology (1950-2007)
Whole Atlantic	**TS + Hur**	**44**	**61**	**58**	**80**	**115**	**144**
	Hur.	**33**	**38**	**45**	**55**	**83**	**93**
	Maj. Hur.	**16**	**21**	**20**	**27**	**59**	**58**
Caribbean Sea	**TS + Hur**	**19**	**19**	**22**	**26**	**41**	**48**
	Hur.	**7**	**13**	**9**	**18**	**22**	**32**
	Maj. Hur.	**6**	**7**	**6**	**8**	**11**	**14**
Gulf of Mexico (all storms)	**TS + Hur**	**23**	**29**	**30**	**39**	**54**	**64**
	Hur.	11	12	17	17	28	27
	Maj. Hur.	7	6	8	7	14	12
Gulf of Mexico (landfalling)	**TS + Hur**	**17**	**19**	**26**	**27**	**42**	**49**
	Hur.	9	8	13	12	19	17
	Maj. Hur.	4	4	4	4	5	4
Southeast	**TS + Hur**	**11**	**12**	**14**	**16**	**20**	**29**
	Hur.	6	6	8	7	14	12
	Maj. Hur.	0	0	0	0	1	1
Northeast	TS + Hur	0	0	1	1	5	5
	Hur.	0	0	0	0	1	1
	Maj. Hur.	0	0	0	0	0	0

Table 6: Full model validation. Variables with at least two P-values significant at the 95% level as determined by Monte Carlo (n = 10,000) simulation are in bold.

Region	Dependent Variable	Hindcast RPSS (1990-2006)	P value	Hindcast RPSS (1980-2006)	P value	LOOCV RPSS (1950-2006)	P value
Whole Atlantic	**TS + Hur**	**0.208**	**0.003**	**0.214**	**0.000**	**0.169**	**<0.001**
	Hur.	**0.112**	**0.036**	**0.122**	**0.007**	**0.056**	**0.003**
	Maj. Hur.	**0.204**	**0.006**	**0.205**	**0.001**	**0.090**	**0.002**
Caribbean Sea	**TS + Hur**	**0.111**	**0.024**	**0.136**	**0.005**	**0.073**	**0.001**
	Hur.	**0.303**	**0.001**	**0.289**	**0.000**	**0.135**	**<0.001**
	Maj. Hur.	**0.158**	**0.027**	**0.156**	**0.010**	**0.094**	**0.002**
Gulf of Mexico (all storms)	**TS + Hur**	**0.107**	**0.034**	**0.079**	**0.029**	**0.049**	**0.008**
	Hur.	0.025	0.146	0.006	0.147	0.003	0.045
	Maj. Hur.	-0.036	0.470	-0.045	0.455	-0.073	0.518
Gulf of Mexico (landfalling)	**TS + Hur**	**0.109**	**0.033**	**0.030**	**0.108**	**0.030**	**0.027**
	Hur.	-0.023	0.428	-0.020	0.363	-0.037	0.341
	Maj. Hur.	-0.059	0.603	-0.086	0.687	-0.121	0.840
Southeast	**TS + Hur**	**0.093**	**0.051**	**0.052**	**0.044**	**0.041**	**0.008**
	Hur.	-0.050	0.329	-0.041	0.239	-0.038	0.128
	Maj. Hur.	-0.051	0.505	-0.050	0.496	-0.059	0.612
Northeast	TS + Hur	-0.062	0.922	-0.107	1.000	-0.087	1.000
	Hur.	-0.176	0.978	-0.309	1.000	-0.085	0.998
	Maj. Hur.	-1.240	0.158	-0.107	0.095	-0.113	0.053

The Caribbean Sea also has significant results for all types of storms, with all nine tests returning an improvement over random chance at 95% significance level. Table 5 shows moderate reductions in error over climatology. Caribbean hurricane predictions are particularly good, with errors reduced by from 0-50% with an average of 24%.

In the Gulf of Mexico (see Table 6), the model shows improvement over random chance at 95% significance level for all named storms passing over the Gulf, but no significant improvement over climatology in the prediction of hurricanes and major hurricanes. In Table 5, the model shows a 15-20% reduction in error for named storms, while hurricanes and major hurricanes show no improvement over climatology. Landfalling storms along the U.S. Gulf Coast are more difficult to predict; the model achieves a gain over random chance at 95% significance level for landfalling named storms for the 1990-2007 hindcast and the LOOCV, but is generally worse than climatology for hurricanes and major hurricanes.

Landfall predictions along the southeastern U.S. coast (Table 6) are at 95% significance level for named storms, but poor for hurricanes and major hurricanes. In Table 5, only the prediction of named storms reduces the error from climatology. The errors for hurricanes are slightly greater than predicting the average 0-1 hurricanes. As far as major hurricanes, because only once in the data record (1955) did more than one major hurricane make landfall in the southeast, predicting 0-1 landfalls is generally accurate. The verification of major hurricanes in Table 5 may have been adversely effected by storms such as Hurricanes Hugo and Andrew, which made landfall along the southeast during years which

are otherwise quiet. The verification of hurricanes is deteriorated by the inclusion of 2007; the verification through 2006 (not shown) is significant at a 95% confidence level in all tests. The 2007 predictions will be covered in more detail.

In the final region, tropical cyclones making landfall along the U.S. northeast from Virginia-Maine, the model performs quite poorly (Table 6.) The Poisson distribution is probably not the most appropriate in this case when events are so rare. In the 1950-2007 data, major hurricanes have only made landfall along the northeast in three years, and none have since 1985. In addition, the regression is likely overfit with only three nonzero values. Table 5 also contains no useful information for the Northeast; predicting 0-1 storms is nearly always correct.

Table 7: 2007 Prediction weights.

Region		Intercept	Nino12	Prin Comp	TSA
Whole Atlantic	**TS + Hur**	2.288	-0.095	0.152	0.119
	Hur.	1.787	-0.106	0.131	0.079
	Maj. Hur.	0.904	-0.198	0.267	0.106
Caribbean Sea	**TS + Hur**	0.732	-0.271	0.265	0.103
	Hur.	0.046	-0.296	0.458	0.149
	Maj. Hur.	-0.493	-0.251	0.363	0.335
Gulf of Mexico (all storms)	**TS + Hur**	1.088	-0.086	0.175	0.159
	Hur.	0.436	-0.183	0.077	0.148
	Maj. Hur.	-0.461	-0.240	0.197	0.133
Gulf of Mexico (landfalling)	**TS + Hur**	0.733	0.004	0.177	0.217
	Hur.	-0.092	0.003	0.046	0.285
	Maj. Hur.	-0.953	-0.035	0.148	0.346
Southeast	**TS + Hur**	-0.077	-0.399	0.271	
	Hur.	-0.563	-0.532	0.195	
	Maj. Hur.	-1.505	-0.458	-0.035	
Northeast	TS + Hur	-0.972	-0.064	-0.026	
	Hur.	-1.886	0.160	-0.105	
	Maj. Hur.	-4.108	-2.114	-0.471	

Table 8: 2007 Predictions and Verification. Numbers of storms predicted by the tropical cyclone activity model for 2007, using April Niño 1+2 prediction and actual Niño 1+2. Note: these predictions do not entirely match the prediction issued in April, 2007 as the methodology has been modified since.

Region		Climatology (1950-2007)	Prediction (using April Niño 1+2 pred.)	Prediction (using actual Niño 1+2)	Actual
Whole Atlantic	**TS + Hur**	**10.10**	**14.07**	**15.08**	**13**
	Hur.	**6.09**	**8.14**	**8.79**	**6**
	Maj. Hur.	**2.64**	**4.46**	**5.13**	**2**
Caribbean Sea	**TS + Hur**	**2.26**	**3.91**	**4.74**	**3**
	Hur.	**1.24**	**2.76**	**3.40**	**2**
	Maj. Hur.	**0.72**	**1.50**	**1.80**	**2**
Gulf of Mexico (all storms)	**TS + Hur**	**3.07**	**4.46**	**4.75**	**5**
	Hur.	1.60	2.11	2.42	3
	Maj. Hur.	0.67	1.07	1.27	0
Gulf of Mexico (landfalling)	**TS + Hur**	**2.16**	**3.07**	**3.06**	**3**
	Hur.	0.95	1.15	1.14	1
	Maj. Hur.	0.41	0.60	0.61	0
Southeast	**TS + Hur**	**1.03**	**1.80**	**2.39**	**1**
	Hur.	0.66	1.08	1.58	0
	Maj. Hur.	0.24	0.28	0.39	0
Northeast	TS + Hur	0.38	0.38	0.40	0
	Hur.	0.16	0.12	0.10	0
	Maj. Hur.	0.05	0.03	0.14	0

d. 2007 Results

The 2007 final prediction model weights and results are shown in Tables 7 and 8. The results of the predictions are mixed. For the entire Atlantic, the model predicted more named storms, hurricanes and major hurricanes (15.08, 8.79 and 5.13, respectively) than occurred (13, 6 and 2). By chance, under-prediction of the strength of La Niña in April compensated for some of the error; in April, 2007 the Jul-Sep Niño 1+2 is predicted to be -0.8, but it actually is around -1.6.

The Caribbean forecast also benefited from the Niño 1+2 forecast error. The April activity forecast is quite good (3.91, 2.76 and 1.50 compared to 3, 2, and 2) while the hindcast predicted the right number of major hurricanes, but one too many tropical storms and hurricanes.

The predictions for overall Gulf of Mexico activity and storms making landfall along the Gulf Coast are some of the best, despite low verification numbers for landfalling storms. In fact, the only error there is that 1-2 major hurricanes are predicted to pass over the Gulf of Mexico, and none did.

The activity predictions for the southeast are the biggest failure of the model. Using the April Niño 1+2 forecast, the model predicts near-normal activity, but with the actual Niño 1+2 that becomes above normal activity for tropical storms, hurricanes and major hurricanes. In reality, only one tropical storm (Gabrielle) made landfall. Many of the tropical cyclones that occurred in 2007 never made it to land.

Predictions for landfall along the northeastern U.S., as discussed above, cannot be trusted. The 2007 predictions display that the model is unstable for that region; with the corrected Niño 1+2 it predicts more major hurricanes (0.14) than hurricanes (0.10). The verifications in Tables 4 and 5 also show that climatology is better than the model in that region.

The issue with the erroneous Niño 1+2 forecast, although it turned out to be helpful in this case, points to another potential weakness of this hurricane forecast. That error has not been included in the validation statistics. Several studies cite the weaknesses of El Niño forecasting (e.g., Barnston et al. 1999, Landsea and Knaff 2000, Halide and Ridd 2008.) In the future, a sensitivity study would be useful to quantify these effects and determine whether or not the presence of an El Niño index explains enough variance in the model to justify the extra error.

e. 2008 Predictions

For 2008, the model predicts a season that is only slightly above normal activity (Table 9.) The only sizable difference from climatology is for named storms over the entire Atlantic, where it predicts 11.39 named storms compared to climatology of 10.10 storms per year.

Table 9: 2008 predictions. Predictions with validations significantly better than climatology at a 95% confidence level are shown in bold.

Region		Climatology (1950-2007)	Prediction (using April Niño 1+2 pred.)
Whole Atlantic	**TS + Hur**	**10.10**	**11.39**
	Hur.	**6.09**	**6.68**
	Maj. Hur.	**2.64**	**3.02**
Caribbean Sea	**TS + Hur**	**2.26**	**2.52**
	Hur.	**1.24**	**1.46**
	Maj. Hur.	**0.72**	**0.88**
Gulf of Mexico (all storms)	**TS + Hur**	**3.07**	**3.55**
	Hur.	1.60	1.73
	Maj. Hur.	0.67	0.75
Gulf of Mexico (landfalling)	**TS + Hur**	**2.16**	**2.58**
	Hur.	0.95	1.08
	Maj. Hur.	0.41	0.50
Southeast	**TS + Hur**	**1.03**	**1.06**
	Hur.	0.66	0.62
	Maj. Hur.	0.24	0.21
Northeast	TS + Hur	0.38	0.37
	Hur.	0.16	0.14
	Maj. Hur.	0.05	0.01

5. Conclusions and Remarks

One of the biggest problems in forming tropical cyclone prediction models is limited historic data. For quality control, early years must generally be eliminated. In this study, using Best Track data from 1944-2007 and climate index data from 1950 forward, left only 58 years of data. Ideally, the data set should be further separated into one section to find predictors and build a model and another on which to test the model. However, with only 58 years of data and some activity cycles on a decadal or longer time scales, one or both of those tasks would rely on inadequate data.

The use of an HTDF and EOFs is a technique for circumventing that dilemma. By maintaining more of the temporal and spatial structure of the Best Track data, they provide quasi-independent data for finding correlated climate indices. Given a set of indices, cross-validation can be used to test the model itself.

The final model generally beats climatology and random chance for basinwide storm counts. Predictions of tropical storms, hurricanes, and major hurricanes in the entire Atlantic Basin show an 11-28% reduction in error from climatology in all but one test. In the Caribbean basin, there is also a significant improvement in the estimation of named storm, hurricane and major hurricane counts versus climatology. Over the Gulf of Mexico the model can predict numbers of named storms better than climatology, but not hurricanes and major hurricanes.

In the prediction of counts of landfalling storms, named storms along the southeastern

coast show the most improvement. That improvement only corresponds with a reduction in prediction error for named storms, where it reduces error by about 10% from climatology. Landfalling named storms over the Gulf of Mexico also improve on climatology. For the northeastern U.S. the model is unstable. Landfalls along the northeast, especially for hurricanes and major hurricanes, are probably too rare in the 1950-2007 record for a successful model.

In 2007, the predictions made by this statistical model are generally too high, especially once a compensating error in the Niño 1+2 forecast is removed. The model particularly over-predicted hurricanes and major hurricanes over the entire Atlantic and tropical cyclones of all kinds making landfall over the southeastern U.S. Named storms and hurricanes are also over-predicted in the Caribbean by about one storm, but the major hurricane prediction verified with two category 5 storms. The Gulf of Mexico, both in terms of all storms passing over the Gulf and storms making landfall along the U.S. Gulf Coast, verified the best in 2007 with all of the landfalling values matching and only the prediction of 1-2 major hurricanes over the Gulf of Mexico being too high.

For 2008, the regression model predicts slightly above normal numbers of tropical cyclones in all of the regions.

APPENDICES

Appendix A: Glossary of variables

AMM: The Atlantic Meridional Mode is the Maximum Covariance Analysis of the SST and the 10m wind field over the tropical Atlantic (Chiang and Vimont 2004.)

AMO: The Atlantic Multidecadal Oscillation is the detrended area-weighted SST across the entire North Atlantic (Enfield et al 2001.)

DM: The Atlantic Dipole Mode (DM) is the standardized SST difference between the North (4°N-24°N, 60°W-15°W) and South (15°S-30°S, 30°W-12°E) tropical Atlantic (Enfield et al 1999; Xie et al 2005a.)

NAO: The North Atlantic Oscillation

Nino: El Niño 1+2 is the area weighted SST anomaly in the eastern Pacific just off the South American coast.

PC: The first principle component of the AMM, AMO, DM, TNA and WHWP indices.

TNA: The Tropical North Atlantic index and is the area-weighted SST anomalies in the North Tropical Atlantic (Enfield et al 1999.)

TSA: The Tropical South Atlantic index is the area-weighted SST anomalies in the South Tropical Atlantic (Enfield et al 1999.)

WHWP: The Western Hemisphere Warm Pool is the monthly anomaly of the area of SSTs > 28.5°C, or warm enough to support a hurricane (Wang and Enfield 2001.)

CHAPTER 2: 2004-2007 Atlantic Tropical Cyclone Activity Comparison

Abstract

This study examines the differences between the four Atlantic hurricane seasons from 2004-07. 2005 had the most favorable SST and vertical wind shear conditions over the main development region. 2004 and 2006 had intermediate levels of SST and wind shear and, outside of the month of August, similar levels of activity. Activity in 2007 was generally suppressed: although more tropical storms formed than in 2006, they were very short-lived. On average, tropical storms in 2007 survived less than 2.5 days.

The strength of the subtropical anticyclone is found to be a very important factor: in 2005, a weak subtropical high allowed for unusually high SST in the main development region, while in 2007 a strong subtropical high over the east Atlantic cooled SST and increased vertical wind shear. The strength of the subtropical cyclone may be related to the heat release of the African monsoon. This finding also emphasizes the importance of factors relating to the strength of the subtropical high pressure in hurricane prediction.

1. Introduction

Since 1995, the Atlantic Basin has been in an active mode for tropical cyclones (TC), an upswing that has been linked to warmer Atlantic SSTs caused by either the Atlantic Multidecadal Oscillation (AMO; Goldenburg et al 2001) or global warming (Emmanuel 2005). Within this active phase there has also been substantial interannual variability. The 2004-07 period is indicative of this variability: 2004 and 2005 were extremely active, 2006 was near-normal and 2007 was below normal in activity. This study investigates the differences in some key fields linked to hurricane initiation and development in the 2004-07 seasons.

Initiation

Of the tropical cyclone life cycle, its initiation is the least understood (Emmanuel 2003). Much of what is known is based on climatologies comparing tropical disturbances that developed with those that did not using cluster analysis. Gray (1968, 1979) describes some necessary but not sufficient conditions for tropical cyclone generation: (1) sufficient low-level relative vorticity, (2) a high enough Coriolis parameter, (3) low vertical wind shear, (4) SST > 26.5°C for the top 60m of ocean (oceanic heat content), (5) a gradient of θe between the surface and 500mb ($\delta\theta e/\delta p$), and (6) high middle tropospheric relative humidity. Later, Gray (1998) proposes a mechanism for the process. Initially, the disturbance is a mesoscale convective system (MCS) with a convective vortex approximately 100 km in radius in the mid-levels. In order to develop, the MCS must also have strong enough winds close to the

center (mean -Vr = -1.3 m/s, Vt = 5 m/s at 55km from center.) In order to continue growing, the storm must then receive some sort of outside influence, which Gray refers to as "externally forced convergence." In the "ignition" phase, extreme convection fires up and the storm transitions from externally forced convergence to internally forced convergence and "extreme convection" begins.

However, the difference between an MCS that develops and one that does not is still the subject of debate. Emanuel (1989) stresses the importance of low-precipitation-efficiency clouds in the initial disturbance that allow convection to moisten the atmosphere without stabilizing it too much. Emanuel (1995) finds in an axisymmetric model the most important condition for further development to be an approximately 100 km-wide column of nearly saturated air near the core of the MCS. Bister and Emanuel (1997) states that along with this moistening of the atmospheric column to discourage downdrafts, the precipitation must be long-lived enough to allow the midlevel vortex to stretch down to the surface.

During the earliest stages of development, strong vertical wind shear may not prevent tropical cyclogensis. Davis and Bosart (2003) determines in a study of baroclinically induced tropical cyclones that 900 – 200-hPa wind shear was initially high (over 10 m s-1) in 8 of the 10 transitioning cases. In 3 cases, the wind shear was initially at least 30 m s-1. Once the tropical cyclones began to develop, it lowered the vertical wind shear in its environment. The strength of the initial disturbances may also play a role. 80% of major hurricanes originated from African Easterly Waves (AEW; Landsea 1993.) Hopsch et al (2007) finds that although western Africa storm tracks do not correlate with TC activity, the strength of

the 2-6 day filtered meridional wind over western Africa does.

Development

Once the TC has become more organized, it can be modeled as a Carnot heat engine (Emanuel 1986, 2003.) As air spirals in toward the low-pressure center of the storm, it draws sensible and latent heat from the ocean below it. That heat drives the pressure lower and strengthens the winds. So long as these conditions continue, the TC should continue to develop up to a theoretical upper bound on its intensity.

Several factors can impede this development. Because the TC is powered by heating from the ocean surface, passing over an area of cooler water can weaken a storm. According to Gray (1968) SSTs of at least 26.5°C are required for hurricane development. Several sources (e.g. Saunders and Harris 1997; Shapiro and Goldenburg 1998) indicate that higher SSTs further promote TC activity.

Vertical wind shear may be an even more important of whether a TC strengthens or weakens. Shapiro and Goldenburg (1998) finds that vertical wind shear explains ~50% of the interannual variability in Atlantic hurricane activity, compared to ~10% for SSTs. Aiyyer and Thorncroft (2006) confirms that seasonal mean VWS explains half of the variability in tropical cyclones within the central main development region (MDR). DeMaria (1996) finds that the inhibitory effect of vertical wind shear is due to the tilting of the TC so that it is not upright. This tilting induces increased warming in the midlevel atmosphere, which in turn disrupts convection. Frank and Ritchie (2001) propose that wind shear causes TCs to tilt via a

top-down, three part process. (1) Wind shear makes the eyewall very asymmetric. (2) High potential vorticity (PV) and equivalent potential temperature (θe) air is mixed outward rather than inward in the upper troposphere where the circulation is weakest. (3) This high PV and θe is advected by the shear, causing the vortex to tilt downshear. Vertical wind shear has a primarily effects in weaker TCs; as a TC strengthens, its own diabatic processes act to decrease vertical tilt (DeMaria 1996.)

The Saharan Air Layer (SAL) also exhibits an inhibitory effect on TC activity. Dunion and Velden (2004) list three reasons for this: (1) the base of the SAL (~800-900 hPa) is extremely warmer than the environmental air, leading to a low-level inversion, (2) dry air entrainment into the TC excites downdrafts and suppresses convection, and (3) the SAL coincides with a jet, causing vertical wind shear. Evan et al (2006) finds a negative correlation between African dust outbreaks and Atlantic TC activity, and proposes that the dust is acting as a tracer for the SAL. Wu (2007) suggests that the relationship between SAL and TC activity may in fact be the link between Sahel rainfall and hurricanes cited in previous studies (Gray 1990; Landsea and Gray 1992.)

The Atlantic dipole mode (DM), defined as the difference between north and south tropical Atlantic SSTs, also correlates with hurricane activity. Xie et al (2005a, b) hypothesizes that DM connects to hurricane activity and location via three primary effects: greater rainfall in West Africa leading to stronger AEW, high SSTs in the MDR, and negative NAO corresponding to a southward shift of the Azores high.

2. Data and Analysis

The hurricane and tropical storm data used here come from the "best-track" database (HURDAT), maintained by NOAA's National Hurricane Center (NHC). SSTs data is NOAA Optimum Interpolation SSTs, which has 1° resolution (OISST, Reynolds et al 2002.) Meridional winds used to find AEW are taken from 1° resolution NCEP GFS analysis. Precipitation is from CMAP data (Xie and Arkin 1996) and plotted by the NOAA/ESRL Physical Sciences Division, Boulder Colorado from their Web site at http://www.cdc.noaa.gov/. NCEP-DOE Reanalysis 2 (provided by the NOAA/OAR/ESRL PSD, Boulder, Colorado, USA, from their Web site at http://www.cdc.noaa.gov/) of 6-hourly winds at 2.5° resolution (Kanamitsu et al 2002) is use for all other atmospheric fields. Track data from 2004-07 is broken down by month to compare when the seasons started, peaked and ended. Where storms formed and how far they traveled is also considered.

The differences which appeared in this analysis are probed by examining several atmospheric and oceanic fields which are believed to influence tropical cyclone genesis and development. For tropical cyclogenesis, SSTs and AEW strength are two important factors. SSTs are plotted as composite anomalies for Jul-Oct, the four busiest months of the hurricane season and the most active months during 2004-07 (see Table 10.) Synoptic AEW strength is explored by plotting the 2-6 day filtered 700 hPa meridional wind between 8°N-20°N from GFS data, which Hopsch et al (2007) found to correlate significantly with Atlantic hurricane activity. The data is filtered via a Lanczos filter (Duchon 1979.)

For further development after the storm has organized, high SSTs, low vertical wind shear and high humidity are keys. Wind shear is shown here in two ways: as composites of Jul-Oct average shear and as the number of days below 10 m s-1, a threshold often used as the maximum shear that a TC can continue developing under (e.g. Frank and Ritchie 2001.)

3. Results

The number of tropical storms, hurricanes, and major hurricanes (Table 10) show that 2005 was by far the most active year; the season was active earlier than the other three years and continued into Dec. It is also notable that although 2004 was far more active than 2006, with the month of Aug removed they have similar numbers of TCs during the hurricane season. 2007 was very quiet aside from a spike in activity in Sep, at the climatological peak of the hurricane season.

2005

A number of factors seem to have contributed to 2005's unprecedented level of TC activity. 2005 has the highest SSTs in the MDR of the four years, and substantially higher SSTs than climatology (Figure 10.) These high SSTs are caused primarily by weaker than normal Atlantic subtropical high in late 2004 and early 2005 (Figure 13.) Anomalously low pressure over the central North Atlantic lead to weakened northeasterly trade winds and a decrease in latent heat loss. This, along with secondary factors of changes in the shortwave radiation budget and horizontal heat advection in the ocean, allowed the western MDR to become unusually warm (Foltz and McFadden 2006.)

2005 also has the lowest MDR vertical wind shear of the four years (6.6 m s-1; Figure 11) and the most days with less than 10 m s-1 VWS (Figure 12.) This may be part of the reason for 2005's large number of hurricanes and major hurricanes (Table 10) as well as the storms lasting longer than in 2006 or 2007 (Table 11.)

Table 10: Number of tropical storms, hurricanes and major hurricanes first observations by month in 2004-07. TCs are grouped according to the month when they first reached that intensity.

		Jun	Jul	Aug	Sep	Oct	Nov	Dec	Jun-Nov
2004	Tropical storms	0	0	8	4	1	1	0	14
	Hurricanes	0	0	5	3	1	0	0	9
	Major hurricanes	0	0	3	3	0	0	0	6
2005	Tropical storms	2	5	5	5	6	3	1	26
	Hurricanes	0	3	2	5	4	0	1	14
	Major hurricanes	0	2	1	2	2	0	0	7
2006	Tropical storms	1	2	3	4	0	0	0	10
	Hurricanes	0	0	1	4	0	0	0	5
	Major hurricanes	0	0	0	2	0	0	0	2
2007	Tropical storms	1	1	2	8	1	0	1	13
	Hurricanes	0	0	1	4	0	1	0	6
	Major hurricanes	0	0	1	1	0	0	0	2
1950-2007 mean	Tropical storms	0.55	0.90	2.79	3.62	1.69	0.53	0.12	10.09
	Hurricanes	0.17	0.38	1.55	2.55	1.07	0.36	0.05	6.09
	Major hurricanes	0.03	0.07	0.64	1.41	0.41	0.07	0.00	2.64

Table 11: Average duration in days of tropical storms, hurricanes and major hurricanes in 2004-07.

	Tropical storms	Hurricanes	Major hurricanes
2004	6.43	5.06	3.71
2005	4.77	3.32	2.50
2006	5.28	4.25	1.00
2007	2.45	2.04	3.00

Table 12: MDR SST and 200-850 hPa vertical wind shear

	2004	2005	2006	2007
MDR SST	0.584	0.907	0.614	0.081
MDR wind shear	8	6.6	8.3	8.5

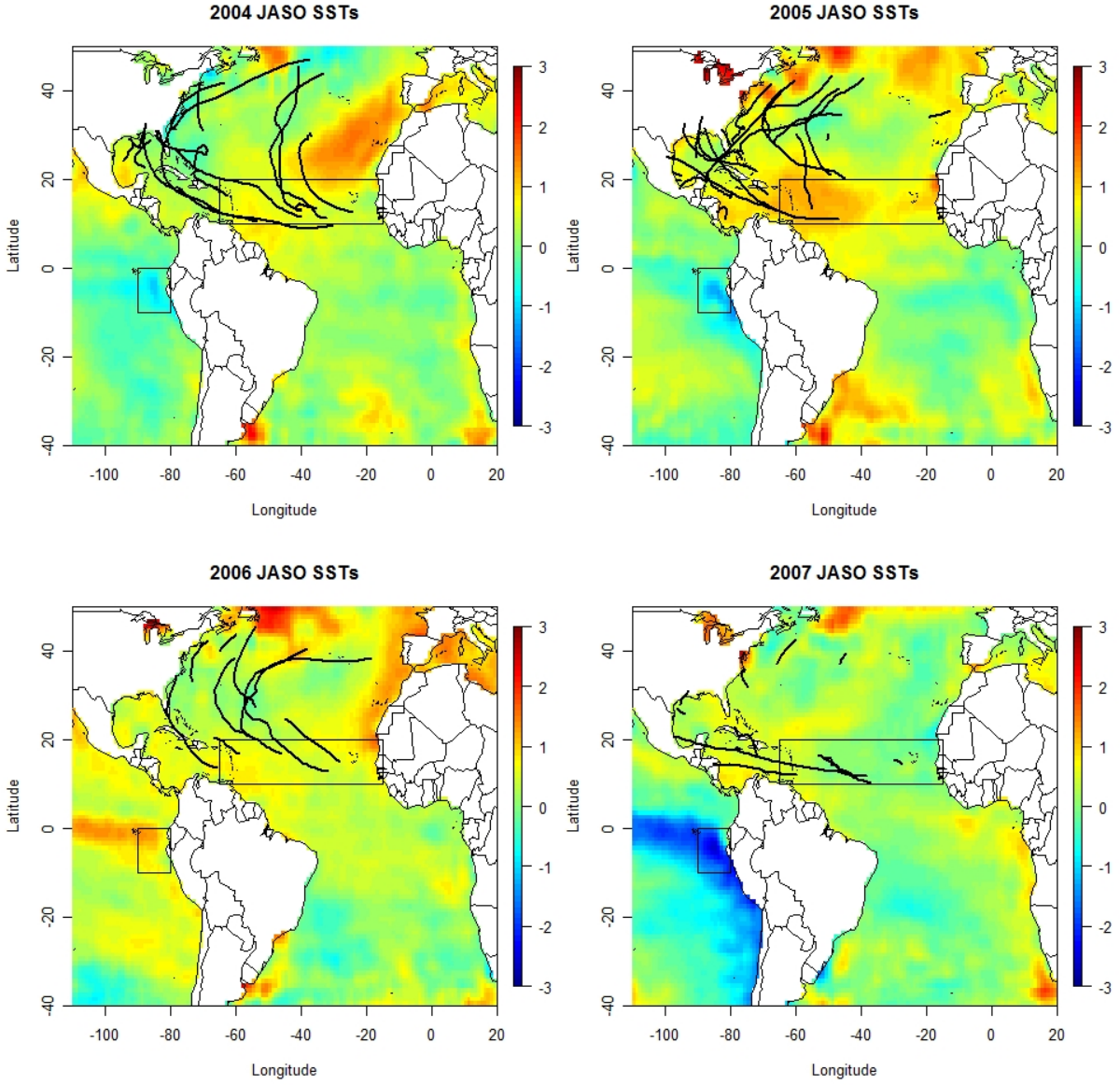

Figure 10: 2004-07 Jul-Oct SST anomalies over the Atlantic and eastern Pacific Ocean. Tropical storm and hurricane tracks for the same period are overlaid in black. The box in the tropical Atlantic is the Main Development Region (MDR; here 10°N - 20°N, 15°W-65°W) and the boxed region in the Eastern Pacific is the Niño 1+2 (10°S - 0°N, 80°W - 90°W)

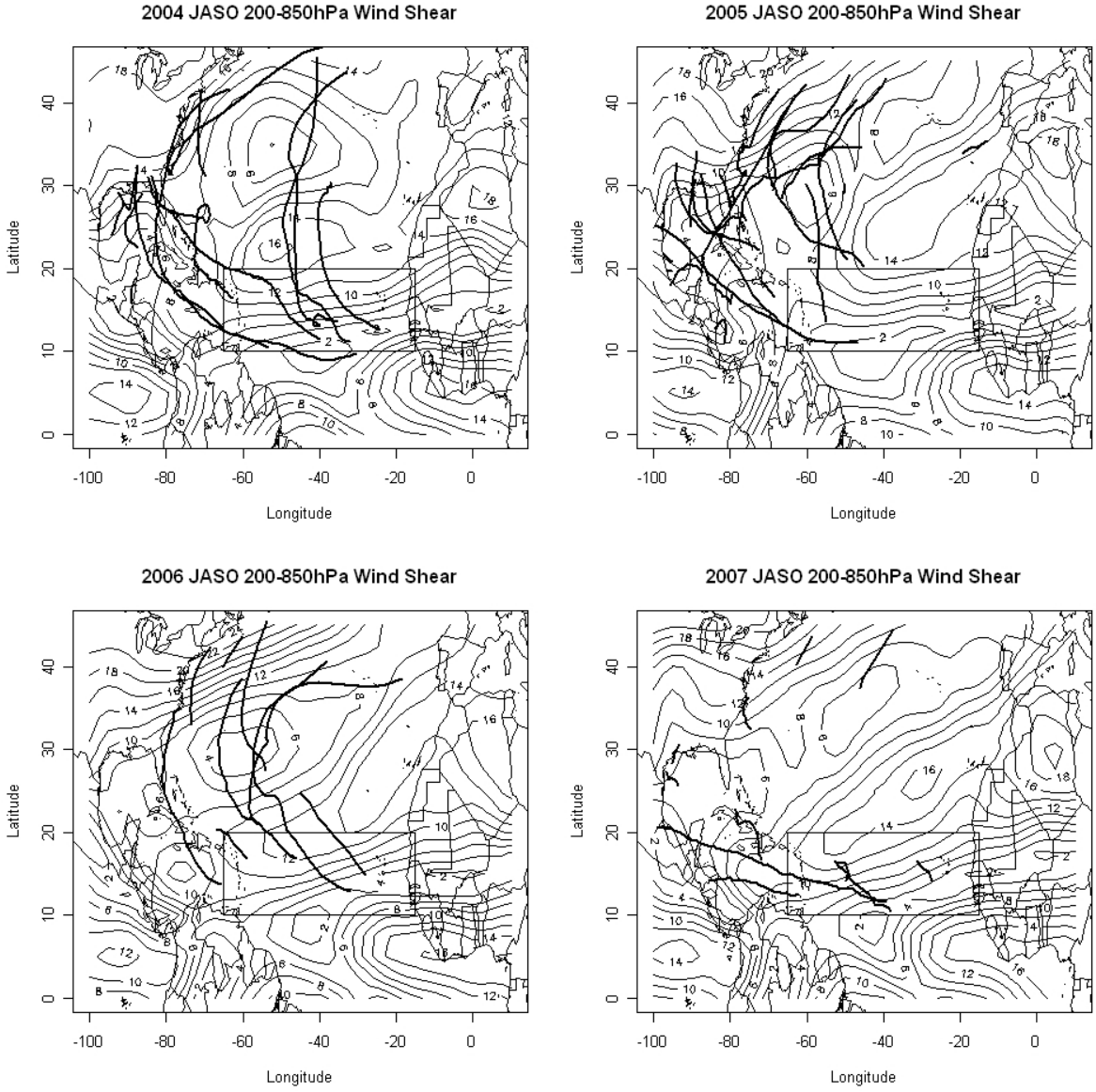

Figure 11: 2004-07 Jul-Oct mean 200-850 hPa vertical wind shear. Values below 10 m s^{-1} are considered conducive to hurricane development. 2005 has the lowest wind shear values over the MDR (6.6 m s^{-1}), followed by 2004 (8.0 m s^{-1}). 2006 (8.3 m s^{-1}) and 2007 (8.5 m s^{-1}) have the highest MDR wind shear.

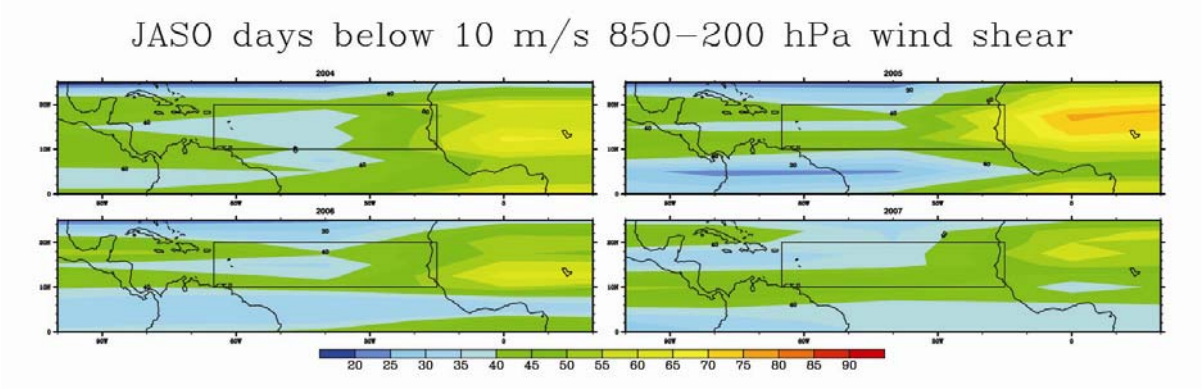

Figure 12: Number of days in Jul-Oct with less than 10 m s-1 wind shear.

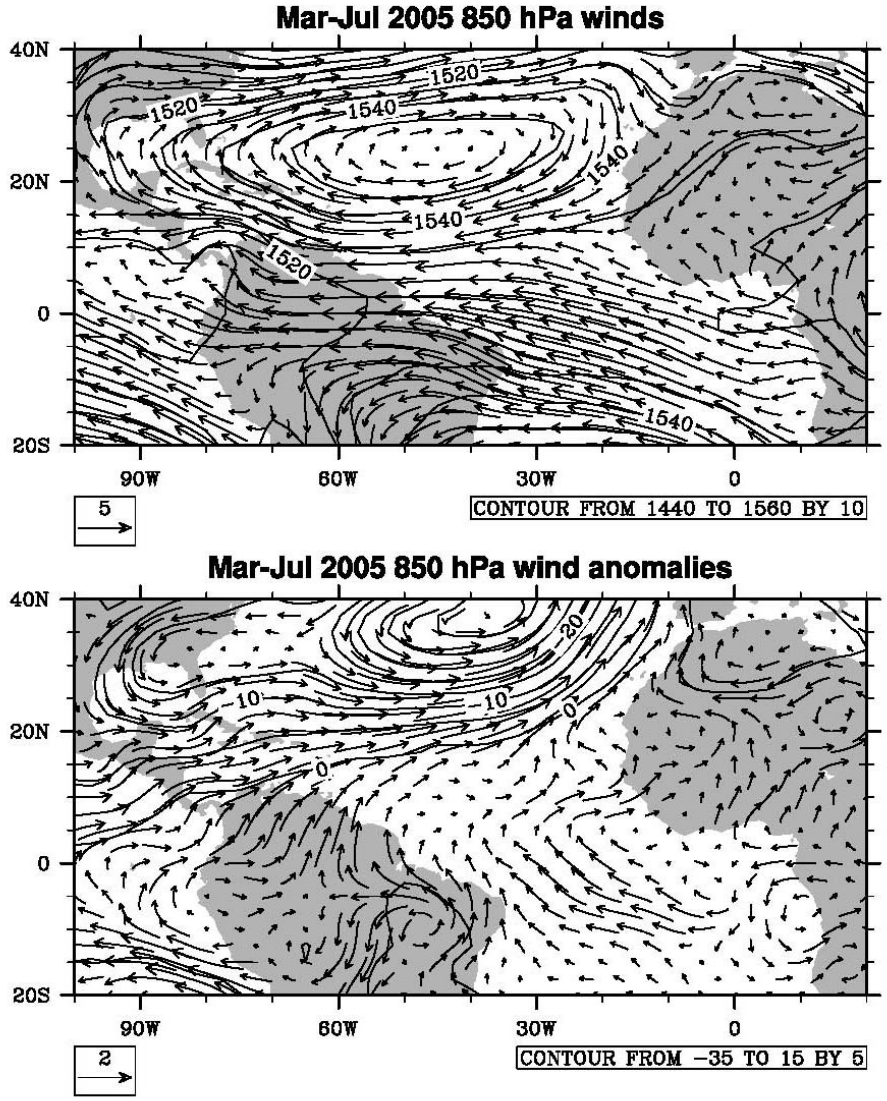

Figure 13: Mar-Jul 2005 850 hPa winds (top) and anomalies (bottom.)

2004 and 2006

2004 is a far more active year than 2006, but if the month of Aug is left out their numbers of tropical storms, hurricanes and major hurricanes are roughly equal; 2004 has 6, 4 and 3 tropical storms, hurricanes and major hurricanes to 2006's 7, 4 and 3. During Aug when the differences between 2004 and 2006 are most pronounced a similar number of AEW exited Africa (Figures 14 and 15.) Yet in 2004 three of the four waves eventually develop into tropical cyclones (one even developed into two systems: H Danielle and TS Earl), while in 2006 only one of three waves develop into TS Debby. Given that similar initial disturbances are passing over the MDR, SSTs and VWS are two likely candidates for the enhanced activity in 2004 relative to 2006.

MDR SSTs are 0.58°C above climatology in 2004 vs. 0.61°C above climatology in 2006 (Table 12, Figure 10.) Vertical wind shear in the MDR is higher in 2006 than in 2004. 2006 is the only year in 2004-07 for which El Niño conditions were present in the eastern Pacific (Figure 10,) which tends to raise VWS over the MDR (Gray 1984.)

2007

Aside from a peak in activity in Sep, 2007 was an extremely quiet hurricane season for the active regime the Atlantic has been in since 1995. Although the TC counts were close to climatology and even higher than the mean number of tropical storms, most of the TCs did not last long; the average duration of tropical storms and hurricanes in 2007 was less than 2.5 days (Table 11.) Only three TCs, major hurricanes Dean and Felix and tropical storm Noel,

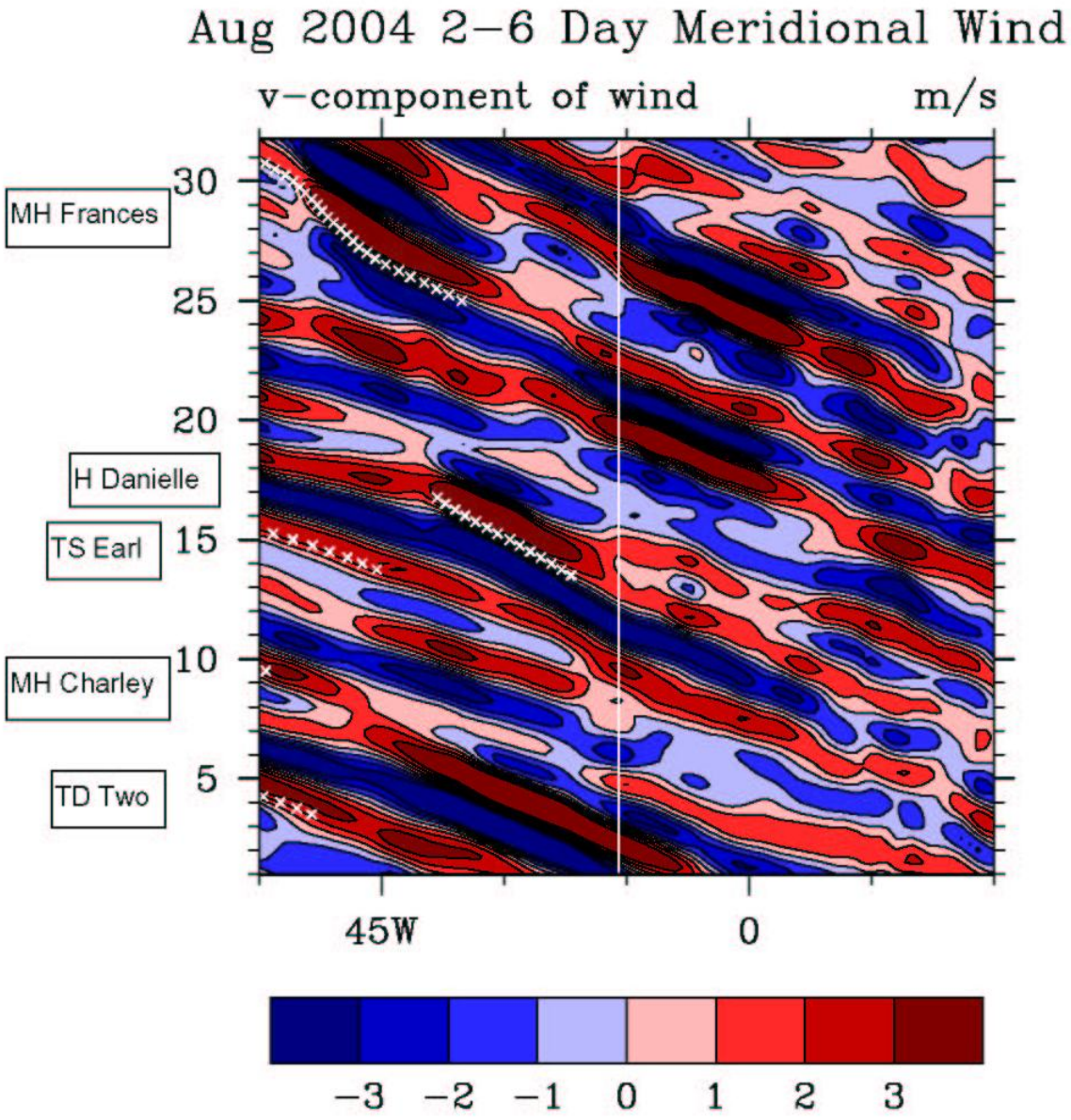

Figure 14: Aug 2004 2-6 day filtered 8°N-15°N meridional wind over Africa and the eastern Atlantic. The at 16°W white line marks the coastline of west Africa.

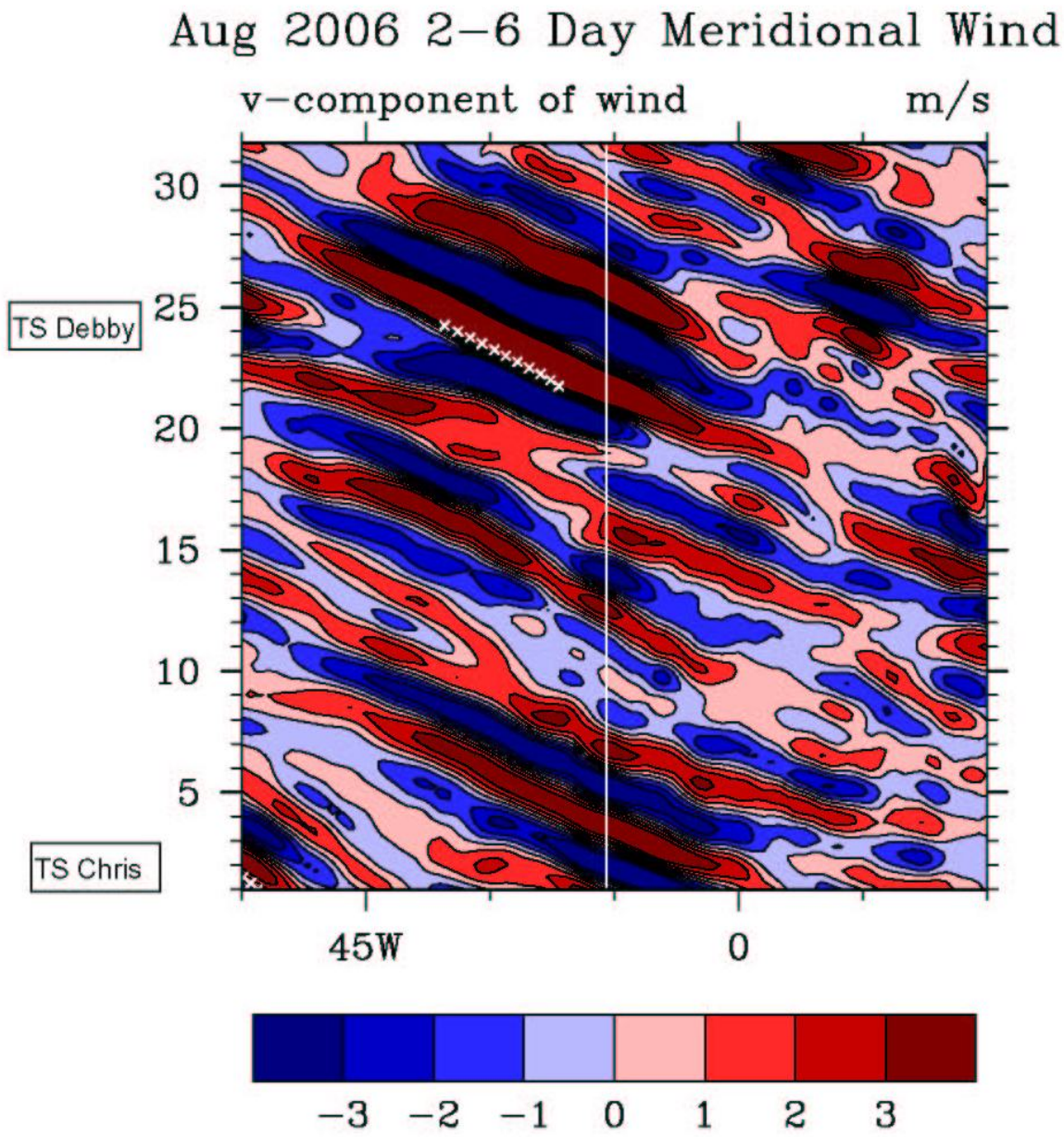

Figure 15: Aug 2006 2-6 day filtered 8°N-15°N meridional wind.

lasted longer than 4 days.

This implies that a factor such as vertical wind shear is at work. TCs were still generated in 2007, but they did not develop for long. 2007 does have the highest mean wind shear of the four seasons at 8.5 m s-1 on average over the MDR. Despite having the strongest La Niña conditions (Figure 10) of the four years, 2007 has the highest average Jul-Oct wind shear in the MDR (Table 12.) Wind shear is particularly high along a SW-NE axis passing through the western MDR; shear is low in the eastern MDR near Africa (Figure 11.)

In the eastern MDR, 850 hPa flow during JASO shows stronger in the westerlies near 10°N, 30°W and moderately increased easterly flow at 200 hPa winds over the same location (Figure 16.) Latent heating from anomalously high SSTs along the Equator near 10°W (Figure 17) incites upward motion (negative omega) and a Rossby wave response to its west, with twin low pressure centers in the North and South Tropical Atlantic near 30°W, as in the modeling study of Wang et al (1996.) This factor intensified the ITCZ near the coast of Africa (Figure 17,) a condition favorable for cyclone development in the eastern MDR. The predominant feature in 2007 appears to be the large geographic extent of the Atlantic subtropical anticyclone (Figure 16). The central portion of the anticyclone is actually weaker than normal, with 850 hPa geopotential heights 12 m below normal. The Mar-Jul 2007 850 hPa wind and geopotential heights (Figure 18) show that the pattern sets up well before the height of the hurricane season.

This strengthened subtropical high over the eastern Atlantic had two primary impacts. First, in a reversal of the conditions that contributed to 2005's record-breaking season, the

northeasterly flow is enhanced, cooling the SSTs near West Africa through increased latent heat loss and coastal upwelling. The anticyclone also enhances the axis of high shear (Figure 11) and contributes to the low number of days below 10 m s-1 VWS in the western MDR (Figure 12.)

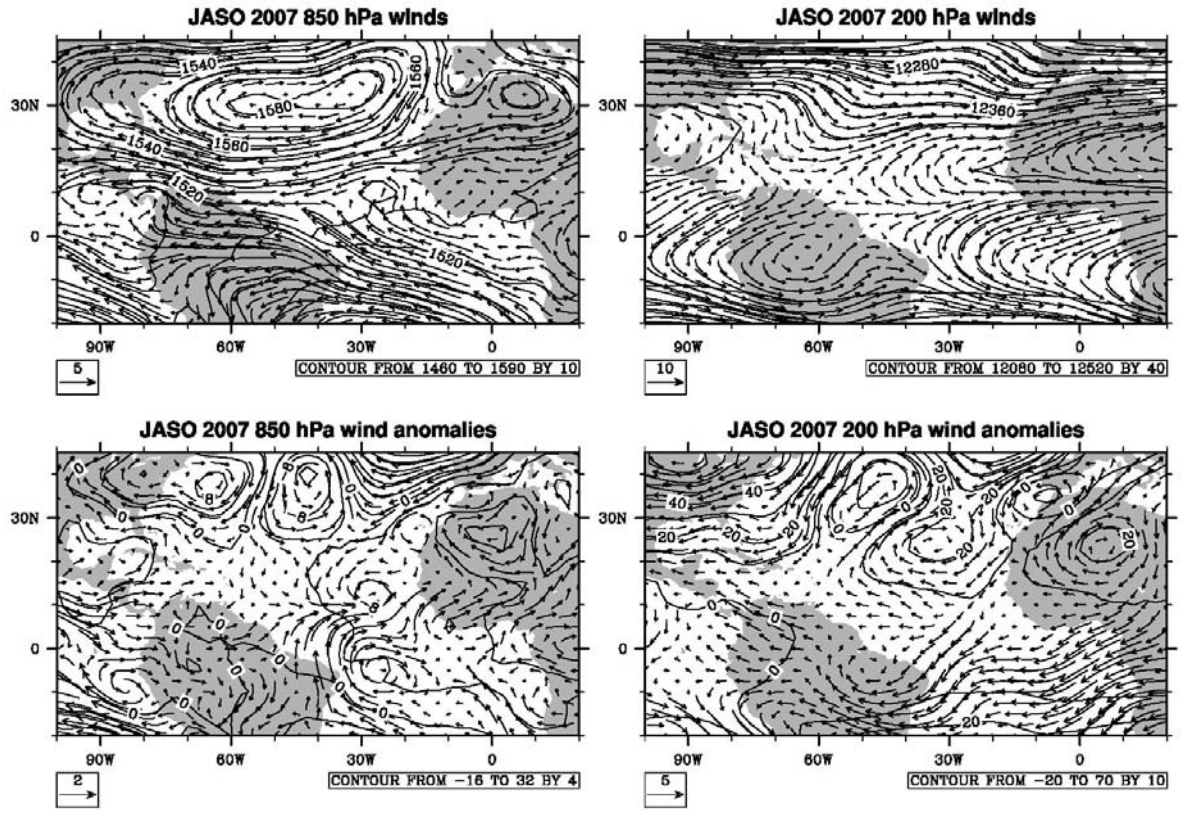

Figure 16: 2007 Jul-Oct 850- and 200-hPa winds with geopotential height contours (top panels) and wind and height anomalies (bottom panels)

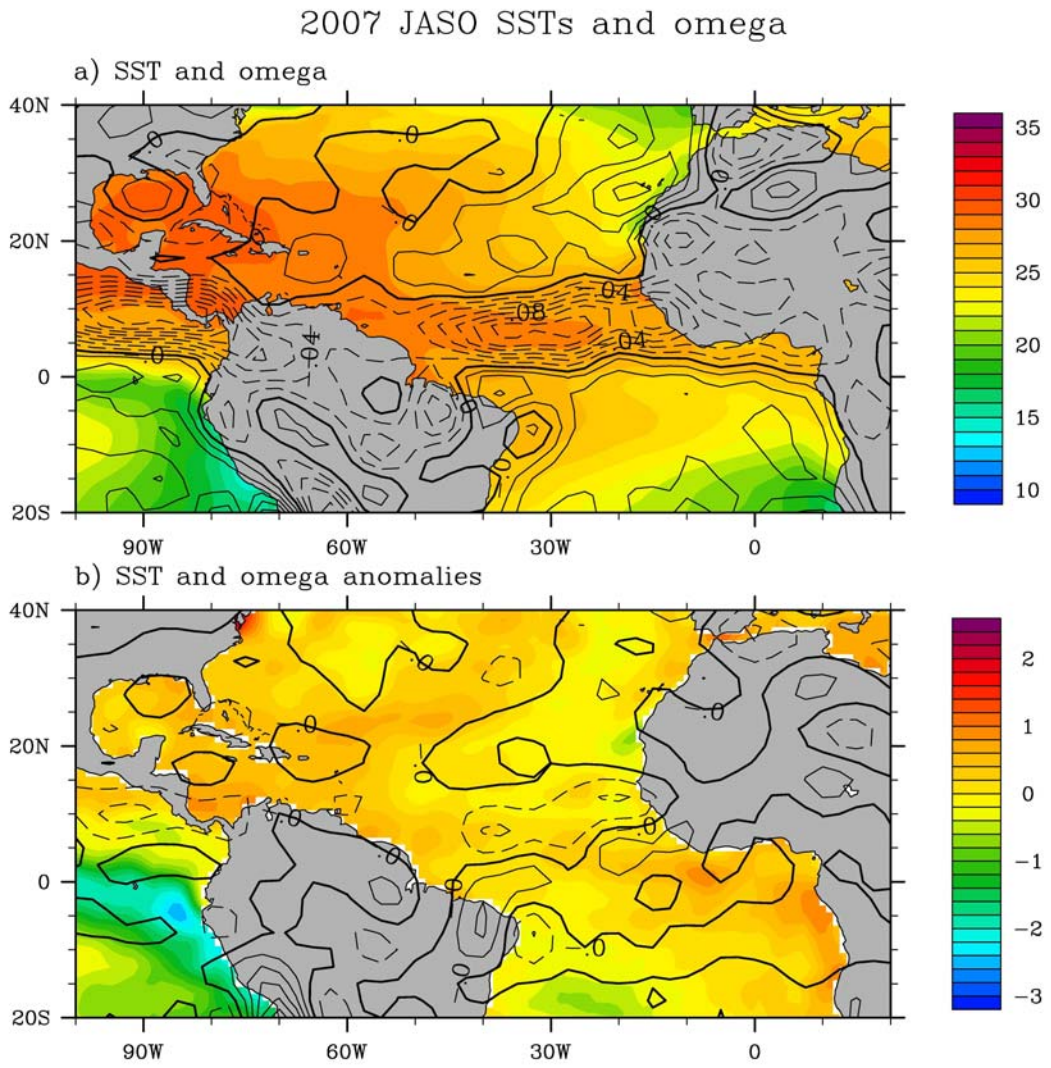

Figure 17: 2007 Jul-Oct 500 hPa omega values overlaid on SSTs. Omega is from NCEP-DOE Reanalysis 2 data, SSTs are OISST data. The top panel shows Jul-Oct mean values, while the bottom panel contains anomalies.

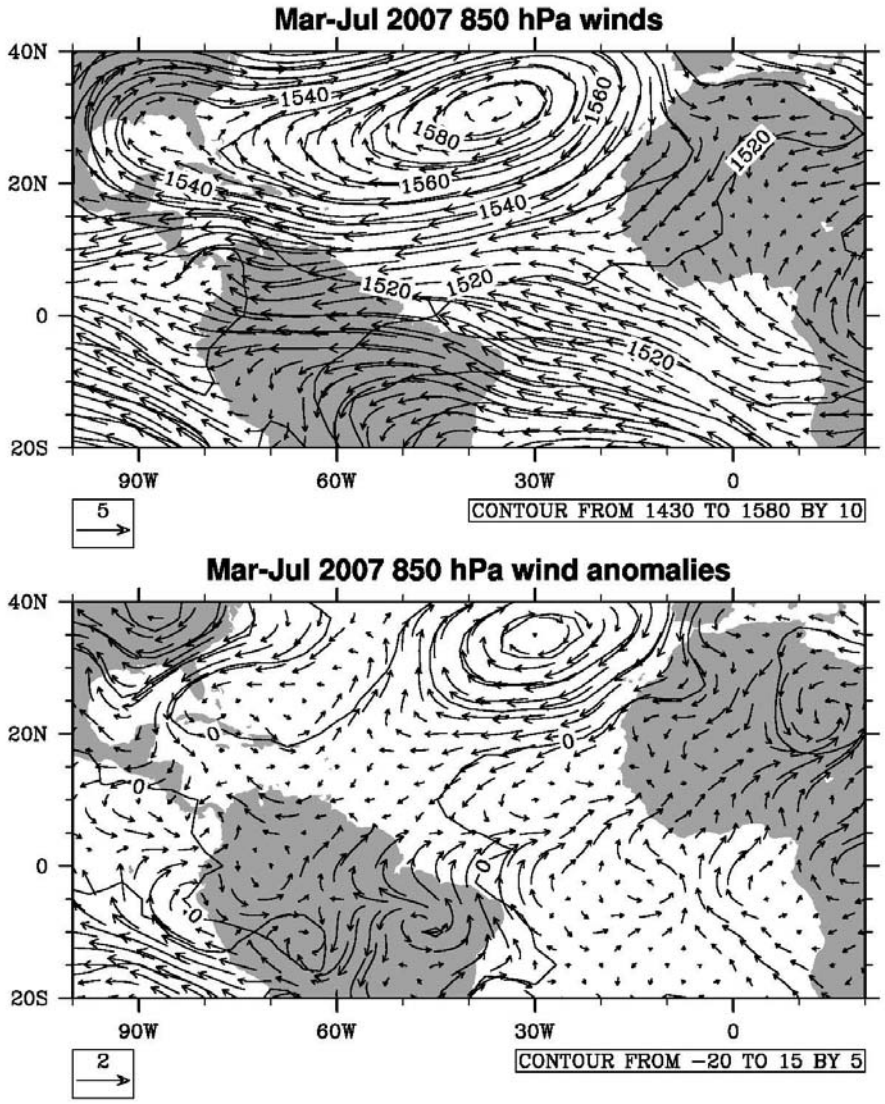

Figure 18: Mar-Jul 2007 850 hPa winds (top) and wind anomalies (bottom.) In a reversal of 2005 conditions at the same time (Figure 4) in 2007 the subtropical high was stronger than normal over the eastern Atlantic, driving stronger northeasterly winds and keeping SST low.

4. Summary and discussion

Although the 2004-07 hurricane seasons all occur during the current active multidecadal mode and have the same potential effects of global warming, they result in vastly different numbers of tropical cyclones over the Atlantic. In 2005, high SSTs and low VWS over the MDR are both favorable for hurricane development. That situation is set up by a weak subtropical anticyclone, which decreased the northeasterly flow over the eastern Atlantic. This, in turn, decreases the latent heat loss of the ocean and the coastal upwelling along West Africa.

2004 and 2006 have intermediate SSTs and VWS of the four years. They are generally similar years except during Aug when 2004 has eight tropical storms to 2006's three. The difference does not appear to be the AEW leaving Africa during that period; the 2-6 day filtered meridional wind has similar numbers and strengths of waves during Aug 2004 and 2006. It may be due to higher VWS in 2006, which agrees with the work of Gray (1984) showing higher VWS during El Niño years.

2007 has more tropical storms than 2006, but it has the shortest-lived storms of any year; on average, tropical storms survive for fewer than 2.5 days. This may be due to the higher VWS and lower MDR SSTs than 2004-06. The high VWS runs counter to the established El Niño response; 2007 has strong La Niña conditions. Both the high VWS and low SSTs can be traced to enhancement of the subtropical high in the eastern Atlantic, which increases the northeasterly winds.

The question then becomes why the subtropical high was extended further east than normal. Hoskins (1996) proposes through theory and an idealized model a linkage between the strength of the eastern part of an oceanic summer subtropical anticyclone and monsoonal activity on the continent to the east. As monsoon heating moves poleward, it enhances descent poleward and westward of it. This descent sets up a feedback; convection is suppressed, negative vorticity is generated and coastal upwelling occurs along the eastern edge of the ocean. All of these serve to further increase descent. Ascent over Africa is balanced by a region of descent over the Mediterranean which stretches west over the eastern Atlantic.

In Jul-Aug 2007, Reanalysis precipitation rate data does show above normal precipitation over Africa (Figure 19.) 500 hPa omega (Figure 20) also shows ascent over Africa with compensating descent over the Mediterranean and eastern Atlantic. The suppression of Atlantic tropical cyclone activity could link to the strength African monsoon.

The importance of the strength of the subtropical high pressure over the eastern Atlantic highlights the importance of a variable relating to it in hurricane forecasting. Both North Atlantic Oscillation (NAO; Elsner 2003) and the Atlantic Dipole Mode (DM; Xie et al. 2005a) are commonly used predictors which correlate with subtropical high pressure strength.

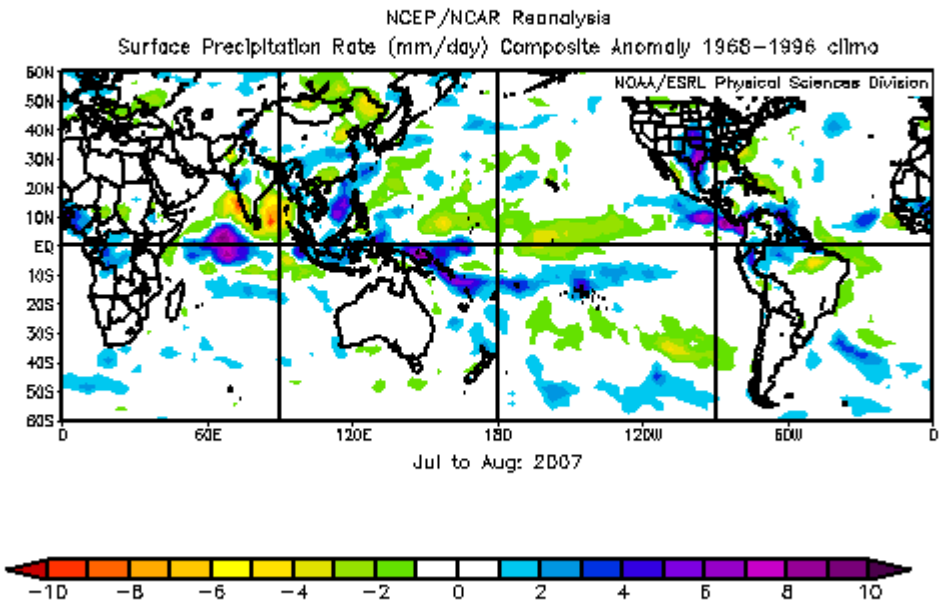

Figure 19: Precipitation anomalies for Jul-Aug 2007. There was above normal precipitation in equatorial Africa during this period. Image provided by the NOAA/ESRL Physical Sciences Division, Boulder Colorado from their Web site at http://www.cdc.noaa.gov/.

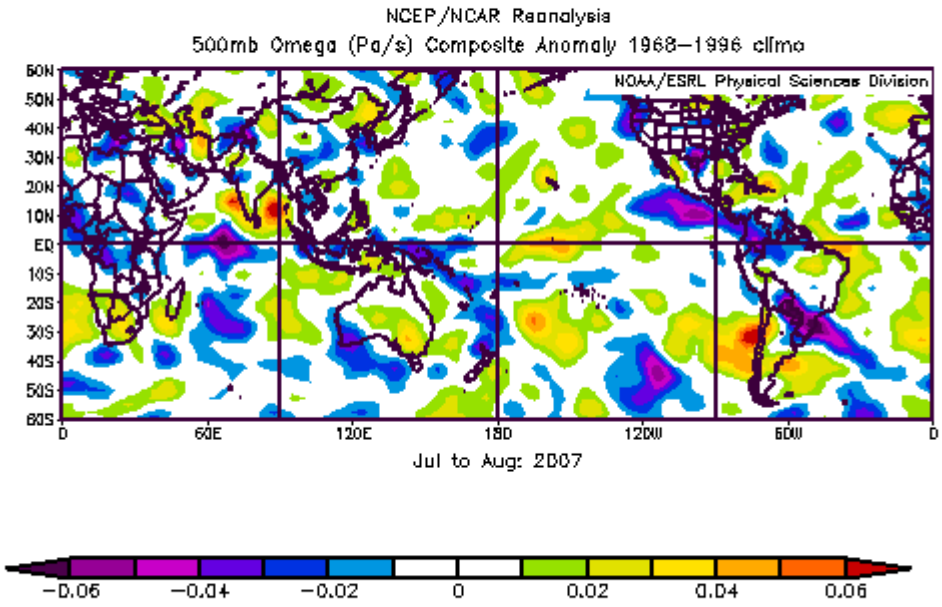

Figure 20: Omega anomalies at 500 hPa for Jul-Aug 2007. Ascent over Africa is balanced by descent over the Mediterranean that stretches into the eastern Atlantic.

REFERENCES

Aiyyer, A. R., and C. Thorncroft, 2006: Climatology of vertical wind shear over the tropical Atlantic. *J. Clim.,* **19**, 2969-2983.

Anderson, J. R., and J. R. Gyakum, 1989: A Diagnostic Study of Pacific Basin Circulation Regimes as Determined from Extratropical Cyclone Tracks. *Mon. Weather Rev.,* **117**, 2672-2686.

Barnston, A. G., M. H. Glantz, and Y. X. He, 1999: Predictive skill of statistical and dynamical climate models in SST forecasts during the 1997-98 El Nino episode and the 1998 La Nina onset. *Bull. Am. Meteorol. Soc.,* **80**, 217-243.

Berry, G., C. Thorncroft, and T. Hewson, 2007: African easterly waves during 2004 - Analysis using objective techniques. *Mon. Weather Rev.,* **135**, 1251-1267.

Berry, G. J., and C. Thorncroft, 2005: Case study of an intense African easterly wave. *Mon. Weather Rev.,* **133**, 752-766.

Bister, M., and K. A. Emanuel, 1997: The genesis of Hurricane Guillermo: TEXMEX analyses and a modeling study. *Mon. Weather Rev.,* **125**, 2662-2682.

Bove, M. C., J. B. Elsner, C. W. Landsea, X. F. Niu, and J. J. O'Brien, 1998: Effect of El

Nino on US landfalling hurricanes, revisited. *Bull. Am. Meteorol. Soc.,* **79**, 2477-2482.

Box, G. E. P., and D. R. Cox, 1964: An Analysis of Transformations. *Journal of the Royal Statistical Society.Series B (Methodological),* **26**, 211-252.

Chelliah, M., and G. D. Bell, 2004: Tropical multidecadal and interannual climate variability in the NCEP-NCAR reanalysis. *J. Clim.,* **17**, 1777-1803.

Chiang, J. C. H., and D. J. Vimont, 2004: Analogous Pacific and Atlantic meridional modes of tropical atmosphere-ocean variability. *J. Clim.,* **17**, 4143-4158.

Davis, C. A., and L. F. Bosart, 2003: Baroclinically induced tropical cyclogenesis. *Mon. Weather Rev.,* **131**, 2730-2747.

DeMaria, M., 1996: The effect of vertical shear on tropical cyclone intensity change. *J. Atmos. Sci.,* **53**, 2076-2087.

DeMaria, M., J. A. Knaff, and B. H. Connell, 2001: A tropical cyclone genesis parameter for the Tropical Atlantic. *Weather Forecast.,* **16**, 219-233.

Demuth, J., M. DeMaria, and J. A. Knaff, 2006: Improvement of advanced microwave sounder unit tropical cyclone intensity and size estimation algorithms. *J. Appl. Meteorol.,* **45**,

1573-1581.

Duchon, C. E., 1979: Lanczos Filtering in One and 2 Dimensions. *J. Appl. Meteorol.,* **18**, 1016-1022.

Dunion, J. P., and C. S. Velden, 2004: The impact of the Saharan air layer on Atlantic tropical cyclone activity. *Bull. Am. Meteorol. Soc.,* **85**, 353-+.

Elsner, J. B., 2003: Tracking hurricanes. *Bull. Am. Meteorol. Soc.,* **84**, 353-356.

Elsner, J. B., and C. P. Schmertmann, 1994: Assessing Forecast Skill through Cross-Validation. *Weather and Forecasting,* **9**, 619-624.

Emanuel, K., 2005: Increasing destructiveness of tropical cyclones over the past 30 years. *Nature,* **436**, 686-688.

Emanuel, K., 2003: Tropical cyclones. *Annu. Rev. Earth Planet. Sci.,* **31**, 75-104.

Emanuel, K. A., 1995: The Behavior of a Simple Hurricane Model using a Convective Scheme Based on Subcloud-Layer Entropy Equilibrium. *J. Atmos. Sci.,* **52**, 3960-3968.

Emanuel, K. A., 1991: The Theory of Hurricanes. *Annu. Rev. Fluid Mech.,* **23**, 179-196.

Emanuel, K. A., 1989: The Finite-Amplitude Nature of Tropical Cyclogenesis. *J. Atmos. Sci.,*

46, 3431-3456.

Emanuel, K. A., 1987: The Dependence of Hurricane Intensity on Climate. *Nature,* **326**, 483-485.

Emanuel, K. A., 1986: An Air Sea Interaction Theory for Tropical Cyclones .1. Steady-State Maintenance. *J. Atmos. Sci.,* **43**, 585-604.

Enfield, D. B., and D. A. Mayer, 1997: Tropical Atlantic sea surface temperature variability and its relation to El Nino Southern Oscillation. *J. Geophys. Res. -Oceans,* **102**, 929-945.

Enfield, D. B., A. M. Mestas-Nunez, D. A. Mayer, and L. Cid-Serrano, 1999: How ubiquitous is the dipole relationship in tropical Atlantic sea surface temperatures? *J. Geophys. Res. -Oceans,* **104**, 7841-7848.

Enfield, D. B., A. M. Mestas-Nunez, and P. J. Trimble, 2001: The Atlantic multidecadal oscillation and its relation to rainfall and river flows in the continental US. *Geophys. Res. Lett.,* **28**, 2077-2080.

Epstein, E. S., 1969: A scoring system for probability forecasts of ranked categories. *J. Appl. Meteorol.,* **8**, 985-987.

Evan, A. T., J. Dunion, J. A. Foley, A. K. Heidinger, and C. S. Velden, 2006: New evidence for a relationship between Atlantic tropical cyclone activity and African dust outbreaks. *Geophys. Res. Lett.,* **33**, L19813.

Evan, A. T., A. K. Heidinger, and M. J. Pavolonis, 2006: Development of a new over-water Advanced Very High Resolution Radiometer dust detection algorithm. *Int. J. Remote Sens.,* **27**, 3903-3924.

Foltz, G. R., and M. J. McPhaden, 2006: Unusually warm sea surface temperatures in the tropical North Atlantic during 2005. *Geophys. Res. Lett.,* **33**, L19703.

Frank, W. M., and E. A. Ritchie, 2001: Effects of vertical wind shear on the intensity and structure of numerically simulated hurricanes. *Mon. Weather Rev.,* **129**, 2249-2269.

Goddard, L., A. G. Barnston, and S. J. Mason, 2003: Evaluation of the IRI's "net assessment" seasonal climate forecasts 1997-2001. *Bull. Am. Meteorol. Soc.,* **84**, 1761-1781.

Goldenberg, S. B., C. W. Landsea, A. M. Mestas-Nunez, and W. M. Gray, 2001: The recent increase in Atlantic hurricane activity: Causes and implications. *Science,* **293**, 474-479.

Gray, W. M., 1979: Hurricanes: their formation, structure, and likely role in the tropical circulation. *Meteorology Over the Tropical Oceans,* D. B. Shaw ed., Royal Meteorology

Society, 155-218.

Gray, W. M., 1998: The formation of tropical cyclones. *Meteorol. Atmos. Phys.,* **67**, 37-69.

Gray, W. M., 1990: Strong Association between West African Rainfall and United-States Landfall of Intense Hurricanes. *Science,* **249**, 1251-1256.

Gray, W. M., 1984: Atlantic Seasonal Hurricane Frequency .1. El-Nino and 30-Mb Quasi-Biennial Oscillation Influences. *Mon. Weather Rev.,* **112**, 1649-1668.

Gray, W. M., 1968: Global View of Origin of Tropical Disturbances and Storms. *Mon. Weather Rev.,* **96**, 669-700.

Halide, H., and P. Ridd, 2008: Complicated ENSO models do not significantly outperform very simple ENSO models. *Int. J. Climatol.,* **28**, 219-233.

Hasanean, H. M., 2004: Variability of the North Atlantic subtropical high and associations with tropical sea-surface temperature. *Int. J. Climatol.,* **24**, 945-957.

Hopsch, S. B., C. D. Thorncroft, K. Hodges, and A. Aiyyer, 2007: West African storm tracks and their relationship to Atlantic tropical cyclones. *J. Clim.,* **20**, 2468-2483.

Hoskins, B., 1996: On the existence and strength of the summer subtropical anticyclones -

Bernhard Haurwitz memorial lecture. *Bull. Am. Meteorol. Soc.,* **77**, 1287-1292.

Kanamitsu, M., W. Ebisuzaki, J. Woollen, S. K. Yang, J. J. Hnilo, M. Fiorino, and G. L. Potter, 2002: NCEP-DOE AMIP-II reanalysis (R-2). *Bull. Am. Meteorol. Soc.,* **83**, 1631-1643.

Knaff, J. A., 1998: Predicting summertime Caribbean pressure in early April. *Weather and Forecasting,* **13**, 740-752.

Knaff, J. A., 1997: Implications of summertime sea level pressure anomalies in the tropical Atlantic region. *J. Clim.,* **10**, 789-804.

Kossin, J. P., J. A. Knaff, H. I. Berger, D. C. Herndon, T. A. Cram, C. S. Velden, R. J. Murnane, and J. D. Hawkins, 2007: Estimating hurricane wind structure in the absence of aircraft reconnaissance. *Weather and Forecasting,* **22**, 89-101.

Kossin, J. P., K. R. Knapp, D. J. Vimont, R. J. Murnane, and B. A. Harper, 2007: A globally consistent reanalysis of hurricane variability and trends. *Geophys. Res. Lett.,* **34**, L04815.

Kossin, J. P., and D. J. Vimont, 2007: A more general framework for understanding Atlantic hurricane variability and trends. *Bull. Am. Meteorol. Soc.,* **88**, 1767-+.

Landsea, C. W., and W. M. Gray, 1992: The Strong Association between Western Sahelian Monsoon Rainfall and Intense Atlantic Hurricanes. *J. Clim.,* **5**, 435-453.

Landsea, C. W., 1993: A Climatology of Intense (Or Major) Atlantic Hurricanes. *Mon. Weather Rev.,* **121**, 1703-1713.

Landsea, C. W., and J. A. Knaff, 2000: How much skill was there in forecasting the very strong 1997-98 El Nino? *Bull. Am. Meteorol. Soc.,* **81**, 2107-2119.

Lorenz, E. N., 1956: *Empirical orthogonal functions and statistical weather prediction.* 48 pp.

R Development Core Team, 2006: R: A language and environment for statistical computing. **2.4.1**

Ramsay, H. A., L. M. Leslie, P. J. Lamb, M. B. Richman, and M. Leplastrier, 2008: Interannual Variability of Tropical Cyclones in the Australian Region: Role of Large-Scale Environment. *J. Clim.,* **21**, 1083-1103.

Rawlings, J. O., S. G. Pantula, and D. A. Dickey, 2001: *Applied Regression Analysis: a research tool.* 2nd ed. 657 pp.

Reynolds, R. W., N. A. Rayner, T. M. Smith, D. C. Stokes, and W. Q. Wang, 2002: An improved in situ and satellite SST analysis for climate. *J. Clim.,* **15**, 1609-1625.

Richman, M. B., and P. J. Lamb, 1985: Climatic Pattern-Analysis of 3-Day and 7-Day Summer Rainfall in the Central United-States - some Methodological Considerations and a Regionalization. *Journal of Climate and Applied Meteorology,* **24**, 1325-1343.

Ritchie, E. A., and G. J. Holland, 1997: Scale interactions during the formation of typhoon Irving. *Mon. Weather Rev.,* **125**, 1377-1396.

Saha, S. and Coauthors, , 2006: The NCEP Climate Forecast System. *J. Clim.,* **19**, 3483-3517.

Saunders, M. A., and A. R. Harris, 1997: Statistical evidence links exceptional 1995 Atlantic hurricane season to record sea warming. *Geophys. Res. Lett.,* **24**, 1255-1258.

Shapiro, L. J., and S. B. Goldenberg, 1998: Atlantic sea surface temperatures and tropical cyclone formation. *J. Clim.,* **11**, 578-590.

Smith, S. R., J. Brolley, J. J. O'Brien, and C. A. Tartaglione, 2007: ENSO's impact on regional US hurricane activity. *J. Clim.,* **20**, 1404-1414.

Smith, T. M., and R. W. Reynolds, 2004: Improved extended reconstruction of SST (1854-1997). *J. Clim.,* **17**, 2466-2477.

Velden, C. S., and L. M. Leslie, 1991: The Basic Relationship between Tropical Cyclone Intensity and the Depth of the Environmental Steering Layer in the Australian Region. *Weather Forecast.,* **6**, 244-253.

Venables, W. N., and B. D. Ripley, 2002: *Modern Applied Statistics with S.* Fourth ed. Springer,

Vimont, D. J., and J. P. Kossin, 2007: The Atlantic Meridional Mode and hurricane activity. *Geophys. Res. Lett.,* **34**, L07709.

Wang, C. Z., and D. B. Enfield, 2001: The tropical Western Hemisphere warm pool. *Geophys. Res. Lett.,* **28**, 1635-1638.

Wang, C. Z., D. B. Enfield, S. K. Lee, and C. W. Landsea, 2006: Influences of the Atlantic warm pool on western hemisphere summer rainfall and Atlantic hurricanes. *J. Clim.,* **19**, 3011-3028.

Wang, T. A., Y. L. Lin, H. F. M. Semazzi, and G. S. Janowitz, 1996: Response of a stably stratified atmosphere to large-scale diabatic forcing with applications to wind patters in

Brazil and the Sahel. *J. Geophys. Res. -Atmos.,* **101**, 7049-7073.

WWRP/WGNE Joint Working Group on Verification, Forecast Verification - Issues, Methods and FAQ. **2007**

Xie, L., T. Z. Yan, and L. Pietrafesa, 2005a: The effect of Atlantic sea surface temperature dipole mode on hurricanes: Implications for the 2004 Atlantic hurricane season. *Geophys. Res. Lett.,* **32**, L03701.

Xie, L., T. Z. Yan, L. J. Pietrafesa, J. M. Morrison, and T. Karl, 2005b: Climatology and interannual variability of North Atlantic hurricane tracks. *J. Clim.,* **18**, 5370-5381.

Xie, P. P., and P. A. Arkin, 1996: Analyses of global monthly precipitation using gauge observations, satellite estimates, and numerical model predictions. *J. Clim.,* **9**, 840-858.